UNIVERSITY OF CALIFORNIA SAN DIEGO

Assessment of Scour Progression using Ultrasonic Guided Waves for Active Scour Monitoring

A Thesis submitted in partial satisfaction of the requirements
for the degree Master of Science

in

Structural Engineering with a Specialization in
Structural Health Monitoring and Non-Destructive Evaluation

by

Prithviraj Rajesh Desai

Committee in charge:

Professor Kenneth J. Loh, Chair
Professor Francesco Lanza di Scalea
Professor Michael D. Todd

2023

The Thesis of Prithviraj Rajesh Desai is approved, and it is acceptable in quality and form for publication on microfilm and electronically.

University of California San Diego

2023

DEDICATION

I dedicate this thesis to my grandparents Narayan Desai (Baba), Konher Sarnobat (Anna Ajja), Ujjwala Sarnobat (Vaini Ajji) and Kamala Desai (Ajji) whose unwavering love, guidance, and inspiration continue to motivate me to go beyond my limits. Their constant support, encouragement, and belief in me have been the driving force behind my academic success. I am forever grateful for their presence in my life, and I hope that this thesis honors their memory and the impact they had on shaping the person I am today. Thank you, Baba, Anna Ajja, Vaini Ajji and Ajji for your unconditional love and for always pushing me to be my best self.

This thesis is also dedicated to my parents, Anjali Desai and Rajesh Desai, who recognized the importance of education and provided me with endless opportunities to engage with intellectual individuals. Their unwavering commitment to my success and their willingness to sacrifice their own comfort and resources have been the driving force behind my academic achievements. Without their support and encouragement, I would not have had the chance to pursue my passions and excel in my studies. I am deeply grateful for their guidance and the love they have shown me throughout my life. Thank you, Amma and Appa, for all that you have done to help me reach this point.

TABLE OF CONTENTS

LIST OF FIGURES

LIST OF ABBREVIATIONS

DO	Dissolved Oxygen
FBG	Fiber-Bragg Grating
FFT	Fast Fourier Transform
HVPA	High Voltage Power Amplifier
MFC	Macro Fiber Composites
MEMS	Micro-Electrical-Mechanical System
NDE	Non-Destructive Evaluation
PVDF	Polyvinylidene Fluoride
PWAS	Piezoelectric Wafer Active Sensors
RMS	Root Mean Square
SHM	Structural Health Monitoring
SOI	Signal of Interest
TDR	Time Domain Reflectometry
UGW	Ultrasonic Guided Waves
UW	Ultrasonic Waves
UTDR	Ultrasonic Time Domain Reflectometry
VTP	Vibration-based Turbulent Pressure

ACKNOWLEDGEMENTS

I am grateful for the guidance and support of my advisor and chair, Dr. Ken Loh, who provided valuable mentorship and professional feedback throughout my time in the ARMOR Lab at UC San Diego. I am also thankful for the opportunities he offered me.

I would like to extend my appreciation to my committee members, Dr. Michael Todd and Dr. Lanza di Scalea, for their contributions and feedback during the completion of my degree. Their assistance was instrumental in helping me achieve my academic goals.

I want to express my gratitude to Elintrix and the U.S. Army Corp of Engineers (USACE). I had a great experience working with Drew Barnett and Dr. Joey Reed. In addition, I appreciate the support of USACE, Dr. Jason Ray, and all other collaborators who contributed to the success of my degree. Special mention to Dr. Koorosh Lotfizadeh (Englekirk) for facilitating the process to perform the on-site installation. The research presented in this dissertation was made possible through funding from the USACE Cooperative Research Agreement No. W912HZ-17-2-0024 and W9132T-22-2-20014.

I would also like to thank my ARMOR Lab colleagues, specifically Chih-Yen Wang, for their support and assistance throughout my program.

Furthermore, I want to express my appreciation to all the friends I met during my time at UC San Diego. Finally, I am grateful to my family, cousins, relatives, and everyone who supported me throughout my master's program. Thank you all for your encouragement and assistance.

VITA

2020 Bachelor of Technology in Civil Engineering, National Institute of Technology Karnataka, Surathkal (India)

2023 Master of Science in Structural Engineering with a Specialization in Structural Health Monitoring and Non-Destructive Evaluation, University of California San Diego (USA)

ABSTRACT OF THE THESIS

Assessment of Scour Progression using Ultrasonic Guided Waves for Active Scour Monitoring

by

Prithviraj Rajesh Desai

Master of Science in Structural Engineering with a Specialization in Structural Health Monitoring and Non-Destructive Evaluation

University of California San Diego, 2023

Professor Kenneth J Loh, Chair

Bridge scour, the erosion of soil around bridge piers, is a leading cause of bridge failures worldwide. The estimation of scour progression is difficult to achieve with available sensor technologies and their reliability during severe flow conditions are questionable. The objective of this study was to demonstrate the concept of a buried-rod scour depth sensor,

where ultrasonic guided waves (UGWs) could be propagated along this waveguide to identify changes in the depth of the soil-water interface levels for determining the state of scour. Previous work already validated the ability to use piezoelectric macrofiber composite sensor-actuators and propagated UGWs along a long thin metal strip as a waveguide for monitoring the soil interface. Building on these foundations, the contribution of this research was two-fold: (1) to enhance the robustness of the sensor design for potential field deployment and (2) to investigate different signal processing methodologies for reliably estimating the soil-water interface or scour depth. First, an H-beam was proposed in lieu of the previous thin aluminum strip. Second, various tests were performed by burying the H-beam in different sediment types and at various depths while assessing the sensitivity of the scour depth sensing methodology to different conditions. A set of signal processing and feature extraction methods were employed to correlate changes in UGWs signal amplitude changes with the soil-interface location along the H-beam. Additionally, the H-beam scour rod was installed in an outdoor test bed to establish the viability of utilizing an UGW-based piezoelectric H-beam to monitor changes in sediment interface.

Chapter 1. Introduction

Many bridges in the United States exceeded their 50-year lifespan or are over 20 years old. Damage and degradation over the years, if not detected or sufficiently repaired, could threaten the continued safety, operations, and serviceability of these bridges. In particular, the risk of bridge collapses is significantly heightened by scour, which has become more frequent due to the impact of climate change on heavy rainfall patterns and flooding. This major factor contributing to bridge collapses, bridge scour, occurs when the flow of a river erodes soil near underwater structures like bridge piers or abutments, resulting in a lowering of the stream bed. This is a common cause of bridge failure worldwide, causing financial losses, transportation disruptions, increased costs, detours, and reconstruction expenses.

Scour events can cause damage to bridges, thus posing a potential threat to public safety. For example, the collapse of the Schoharie Creek Bridge in 1987 was caused by scour at the bridge's foundation, which undermined the bridge's structural integrity. The heavy rainfalls and floods that occurred during the time of the incident worsened the scour, leading to the eventual collapse of the bridge leaving 10 people dead. Scour occurs in three main forms, namely, general scour, contraction scour, and local scour. One among them, local scour (Figure 1) around a bridge pier occurs when fluid downflow at the face of the pier begins to erode sediments at its base, which jeopardizes the integrity of the foundation [1-2]. Figure 2 shows the current's downward flow upon reaching the pier face during local scour, with horseshoe vortices forming and magnifying to deepen the scour hole upstream. According to Arneson *et al.* [3], 60% bridge failures in the United States were a result of scour. In fact, scour-induced failure was identified as the leading cause of most hydraulic collapses [3-4].

During the last 30 years, 600 bridges have failed due to scour problems [5]. In one study of the 500 bridge failures that occurred in the United States between 1989 and 2000, flooding and scour were the cause of 53% of the recorded failures [6]. During a single flood event in 1993 and in the upstream Mississippi and downstream Missouri river basins, at least 22 of the 28 bridges failed due to scour. The associated repair costs were more than USD $8 million [7]. With climate change leading to longer and more severe rainy seasons, it is projected that within the next 75 years, 90% of bridges located in the Southwestern United States will become vulnerable to scouring [8]. Besides, in the event of an extreme flow occurrence, the foundation of a structure may be compromised, even if the superstructure remains intact. This compromised foundational system may appear unaffected, yet still pose a significant risk to the structure's overall stability [9-10]. The monitoring of bridge scour is crucial as it plays a key role in ensuring bridge safety. As a result, early detection of potential scour-related problems through bridge scour monitoring is of utmost importance to ensure the safety of bridges. providing valuable insights into the scouring process, and aiding in understanding the mechanism behind it.

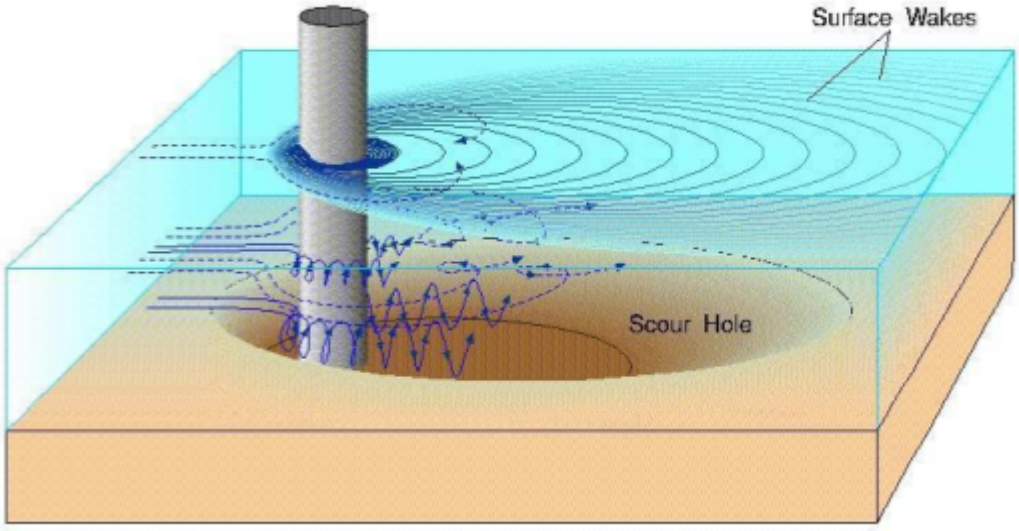

Figure 1. Representation of the local scour hole near bridge pier due to water flow [1].

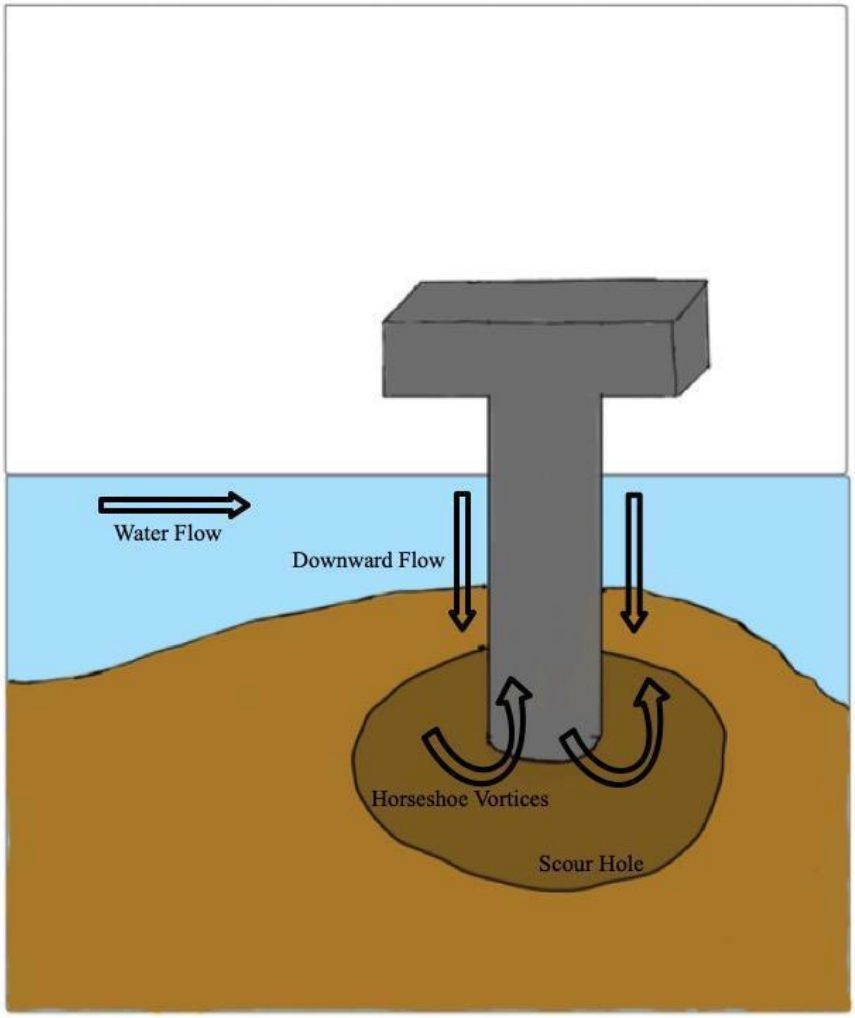

Figure 2. The illustration shows the current's downward flow upon reaching the pier face during local scour, with horseshoe vortices forming and magnifying to deepen the scour hole upstream.

1.1 Current State-of-the-Art in Scour Monitoring

Laboratory experiments and field studies for the prediction of local scouring have faced difficulties in accurately replicating and measuring this phenomenon [9-10]. In the past, scour monitoring has been primarily conducted through visual inspections, typically carried out by divers who assess the bridge foundations. The frequency of these inspections varies depending on the bridge owner and quality, with the National Bridge Inspection Standards prescribing a maximum interval of up to five years [11]. However, this approach poses significant safety hazards to the divers involved and is not feasible during floods, which is when foundations are most susceptible to scour. It also involved infrequent measurement periods and the requirement for an on-site technician. Another technique involves the use of sounding rods or ropes that are inserted near the bridge piers to measure the depth of the riverbed. This method also involves human efforts in a periodic manner. Another alternative was to use boat or raft sonar to map the entire scour topography, but this method also required a technician and was not performed regularly. The older contemporary scour monitoring methods involving human personnel for bridge scour have limitations that can impact the accuracy and efficiency of detecting scour alongside the safety of the personnel. In light of the significant concern surrounding scour for the bridge piers and foundations, significant strides have been taken to innovate technology-driven tools and sensors, enabling the monitoring of scour progress with enhanced efficiency and understanding.

Efforts have been undertaken to predict scour rates and maximum scour depths based solely on soil properties [12]. As technology continues to evolve, it is important to explore new approaches that are more reliable, cost-effective and require less human intervention. In

the course of years, many methods for real-time scour monitoring were studied, such as using float-out devices [13], electrical resistance sensors [14-15], optical fiber sensors [16-17], acoustic/vibration sensors [18-19], fiber bragg grating (FBG) [20], ground-penetrating radar [21], and green laser [22]. Each technique has its own operational conditions, advantages, and limitations. For example, the float out devices were submerged underwater and buried beneath soil. When their location was breached, these devices would float to the surface. While this approach eliminated the need for a technician, the sensors still required reburial after each exposure event. A float-out device is limited to only monitoring the maximum scour depth, and the device's integrity or battery condition cannot be examined after installation. Although the laboratory experimental validations and small scale tests of these sensors were successful, not many of them are robust enough to be deployed in a real environment. Thus, it became essential to develop sensor systems that can be reliable as well as field deployable.

1.2 Modern Technologies

In recent years, numerous inventive solutions have emerged to effectively monitor scour and its effects on bridges. These solutions aim to provide more accurate and comprehensive information, enhancing our understanding of local scour phenomena. By leveraging these advanced techniques, researchers and engineers can make informed decisions to improve bridge safety and maintenance practices. Some of them are (i) tilt sensors (ii) magnetic collar-driven (iii) smart rocks (iv) stack or buried sensors (v) time-domain reflectometry (TDR) sensors and (vi) dissolved oxygen (DO) sensors. Field testing has

demonstrated the significant advancements of these sensor systems compared to previous technologies

Tilt sensors are devices that measure the tilt or inclination of an object. In scour monitoring, they are installed on structures vulnerable to scour. Tilt sensors use accelerometers or gyroscopes to detect changes in orientation and convert them into electrical signals. They are used for measuring changes in the angle of a bridge superstructure after scour has occurred. However, tilt sensors can also detect normal bridge vibrations that are not related to scour, which complicates the estimation of scour. As a result, these sensors may provide a warning later than other sensors that have already detected a change [23].

The magnetic collar-driven technique is a non-invasive method for monitoring scour in bridge foundations. It involves installing a magnetic collar around the bridge pile and monitoring any changes in the magnetic field. As the scour hole around the pile deepens, the magnetic field changes, which is detected by sensors on the collar. This allows for real-time monitoring of the scour depth. The magnetic sliding collar triggers the closure of magnetic switches along a rigid rod as gravity pulls the collar past its location [24]. One potential drawback of the magnetic collar-driven technique is that it may not work well in certain soil conditions or with certain types of bridge foundations.

Smart rocks are a type of scour monitoring technique that involves placing small sensors inside rocks near a bridge foundation [25]. These sensors can detect changes in water pressure and send signals wirelessly to a nearby receiver, which can be used to monitor scour in real-time. Smart rocks have been shown to be effective in detecting scour and have been tested on several bridges [25]. The idea behind these untethered sensors is that they can roll to

the deepest point in a scour hole and are not limited by battery life; magnetic fields are permanent. Two types of smart rocks were developed that both contained magnetic components; a smart rock with direction-unknown where the magnet was oriented based on the position of the rock, and direction-known where the magnet was always oriented to the direction of the ambient magnetic field [26]. However, there are some limitations to the use of smart rocks for scour monitoring. For example, they may not work well in fast-moving water or in areas with high levels of sediment. In addition, the sensors may need to be replaced periodically, which can be costly and time-consuming. Furthermore, the cost of installing and maintaining the necessary equipment for receiving and interpreting data can be expensive.

Various types of stack/rod sensors have been developed for monitoring bridge scour and riprap effectiveness. These include vibration-based turbulent pressure sensor (VTP), housed accelerometer stacks, discrete micro-electrical-mechanical system (MEMS) type sensors, discrete piezoelectric film sensors, dissolved oxygen (DO) sensors, and vibration-based cantilever rods. The VTP uses a rigid pipe with multiple gaps, each containing a thin plate attached to an accelerometer, to detect turbidity in the water of a scour hole [27]. By analyzing the total energy response of each plate, the VTP can determine if it was exposed to flow or buried. A VTP stack was installed near a bridge pier and powered using solar cells [28]. However, the device was dislodged and damaged twice during two flooding events within a year. Although the device was eventually reinstalled and remained in place during flooding events, debris accumulation in front of the sensors hindered the results [29]. It may be possible to alleviate debris accumulation by rotating the device so that the sensors do not face the direction of oncoming flow.

Accelerometer stacks housed in steel cases are another type of sensor that utilize the vibrations induced by flowing water to detect scouring. The accelerometer is placed along the length of a bridge pier and is surrounded by silicon, making it more robust in the unpredictable underwater environment [30]. Unlike VTPs, housed accelerometer stacks are placed in a steel case to provide additional protection. In the field, the accelerometer stacks are housed in steel balls that are surrounded by a cage. This system has proven to be sturdy enough for permanent installation on the Min-Chu Bridge in Taiwan [31]. Alternatively, MEMS type sensors can be used to monitor the underwater environment. These devices are composed of micromachined sensors, actuators, mechanical elements, and electronics to create small electro-mechanical devices [32]. Instead of using accelerometers, MEMS type sensors can be used to monitor exposure to the underwater environment [33].

Fiber optic probes with an oxygen-sensitive coating are used as dissolved oxygen (DO) sensors. These probes detect the presence of oxygen in water by measuring the luminescence emitted from a light-emitting diode near the optical fiber, which decreases as the amount of oxygen present increases [34]. DO sensors are installed at discrete locations along the pier where scour increases the amount of DO present in sensors that are uncovered by the water. Although initial flume studies have shown the functionality of these sensors, their sensitivity to factors such as biological activity, biofouling, and water turbidity has not been investigated. A comprehensive comparison of the advantages, disadvantages, limitations, and relative costs of the above mentioned instruments for measuring bridge scour was presented by Lu *et al.* [35].

Another popular scour monitoring method being utilized in current research is time domain reflectometry (TDR). TDR sensors are stationary sensors that use an energy packet, such as light, sound, or electricity, to detect changes along a sensing element [36-39]. These sensors measure the time it takes for the energy to travel from a transducer to a specific point of interest and then return, allowing them to monitor and detect changes in the sensing element's length. Dowding *et al.* [40] described one of the initial field-deployable TDR systems for bridge scour monitoring. Yankielun *et al.* [41] developed a rugged TDR sensor made of steel pipe and can be permanently installed under the riverbed. This sensor has been installed at several locations to monitor the extent of scour surrounding bridge piers. Yu *et al.* [42] assessed another TDR system under laboratory conditions. Although ultrasonics and TDR are among the emerging technologies for scour monitoring, several other techniques have been suggested. However, there is still a necessity to overcome the limitations of these techniques and develop a cost-effective yet efficient solution.

1.3 Research Objectives

In the light of the inherent challenges associated with accurately measuring scour depth using current scour sensors without compromising their functionality during operational conditions, a new concept based on embedding a rod in soil was proposed by Azhari and Loh [43] by developing a scour sensor based on a slender piezoelectric polyvinylidene fluoride (PVDF) thin film encased in a flexible rod (piezo-rod), which mitigates drawbacks from the existing and emerging technologies. The piezo-rods could be buried systematically in locations surrounding a bridge pier. The electromechanical properties of PVDF allowed these types of sensors to output voltage time histories when subjected to hydrodynamic excitations

from flowing water. The voltage time history data were then acquired, processed, and analyzed for its instantaneous fundamental frequency of vibration, whereby the length of the piezo-rod (i.e., scour depth or exposed length of the rod) was directly calculated. Using a network of these sensors, sediment depth at different locations were plotted spatially to produce a scour topography map. The passive nature of piezoelectric transducers was ideal for scour monitoring, since it generates a voltage in response to strain, thus eliminating the need for an external power source. Although the tests showed that the piezo-rods generated good voltage response, a wide spread of identified frequencies were found in areas where sensors underwent less excitation.

To work on the drawback of the piezo rod proposed earlier, newer generation scour sensor rods were developed by Funderburk *et al.* [37-38]. The studies validated a previously developed passive, vibration-based piezoelectric driven-rod sensor under simulated scour conditions with varied flow velocities. These sensors minimized the effect of flow velocity while increasing the scour sensitive features present in the signal signature. Additionally, a new concept called ultrasonic time domain reflectometry (UTDR) sensing mechanism was utilized to detect soil interfaces through an actuator-sensor pair. The sensor rod employed in this study comprised a thin, slender aluminum strip equipped with two sensors positioned on its surface, serving as both actuator and sensor. The sensing mechanism employed in this system was ultrasonic time-domain reflectometry (UTDR), which enabled the detection of localized pressure distribution on the strip caused by weights and the interface between compacted and uncompacted soil. The strip was horizontally placed beneath the soil for testing purposes. This solution offered distinct advantages over other existing and emerging scour monitoring methods. Piezo-rods can be systematically embedded in the areas

surrounding a bridge pier to detect scour activity and provide valuable information about scour depth and sediment distribution.

This thesis investigates the concept of a buried-rod scour sensor, where ultrasonic guided waves (UGWs) could be propagated along this waveguide to identify changes in the depth of the soil-water interface levels for scour assessment and monitoring. The use of UGWs in scour monitoring offers several benefits, including the ability to use just a sensor-actuator pair at one end to probe for the location of the soil-water interface along the entire length of the waveguide structure. A robust design prototype was proposed in this study involving the use of an aluminum H-beam that can be driven into the soil bed. Piezoelectric sensors can be employed to transmit Lamb wave ultrasonic pulses, allowing for extended distance monitoring of response signal changes. The thesis also validates the functionalities of the piezoelectric sensors for active monitoring of the local scour at bridge piers. The methods presented in this study combine the signal processing with the UGWs methodology. A time-of-flight method using cross-correlation was proposed for better results compared to previous study done by Funderburk *et al*. [37]. Additionally, the newly proposed feature extraction method using convolution provides a continuous assessment of the scour process. The process of the feature extraction method greatly reduces the requirement for complex electronics and signal processing techniques that are typically necessary for conventional ultrasonic investigations. The proposed prototype has been designed for improved durability, measurement sensitivity, and practical field installation. This study also presents a pilot field test that was conducted to provide a solid foundation for the practical implementation of UGWs scour monitoring in the field.

Chapter 2. Background

2.1 Ultrasonic Guided Waves

Ultrasonic waves (UW) are typically produced using a transducer that converts electrical energy into mechanical vibrations. These vibrations propagate through a medium, such as air or water, and when they encounter an object or boundary in the medium, some of the energy is reflected back to the transducer. This reflection creates an echo that can be detected and analyzed to provide information about the object or boundary, such as its distance or composition. This process is commonly used in a variety of applications, including medical imaging, industrial testing, and underwater navigation. By analyzing the echoes generated by ultrasonic waves, it is possible to obtain detailed information about the properties and condition of the medium and the objects within it.

In the field of ultrasonics, the parameters of velocity and attenuation are crucial for analysis. The velocity of longitudinal waves in solid materials can be determined based on the material's properties by Eq. 1:

$$v_L = \sqrt{\frac{\gamma + 2G}{\rho}} \tag{1}$$

where γ is Lame's constant, G is the modulus of rigidity, and ρ is the density. Lame's constant and the modulus of rigidity are related to the elastic modulus, E, and Poisson's ratio, ν, by Eq. 2 and Eq. 3:

$$\gamma = \frac{\nu E}{(1+\nu)(1-2\nu)} \tag{2}$$

$$G = \frac{E}{2(1+\nu)} \tag{3}$$

On the other hand, ultrasonic guided waves are a type of ultrasonic wave that is confined to propagate along the surface of a structure. In other words, UGWs refers to a family of waves that propagate along the length of a structure, such as a pipe or a rail, guided by its boundaries. These waves can be guided in different ways, including through the use of a particular mode or by exploiting the interaction of waves with structural features. It is important to recognize that the method of UGWs differs significantly from the conventional ultrasonic wave method (Figure 3). In the UW method, the wave propagates in a limited area and experiences quick attenuation, resulting in a relatively limited sensitivity range. To inspect the condition of a long pipe using the UW method, the transducer location must be shifted the structure. However, in UGWs testing, stress waves with a low frequency propagate the pipe and experience slower attenuation [44]. As a result, UGWs testing allows for longer without the need for frequent transducer repositioning. UGWs are used in a wide range of industrial applications, including structural health monitoring, non-destructive testing and defect detection. One of the primary advantages of using UGWs is their ability to propagate over long distances while remaining confined within the structure. This allows for the detection of defects or damage that may not be easily visible or accessible from the surface. For example, in pipeline inspection, guided waves can be used to detect corrosion or defects in inaccessible areas, such as underground or under insulation. In addition, guided waves can be used to inspect large areas quickly and efficiently, reducing the need for time-consuming and costly manual inspections. UGWs are generated using transducers, which are typically placed on the surface of the structure. The transducer produces a mechanical vibration that propagates along the surface of the structure, creating a guided wave. The wave can be excited using a variety of methods, including pulse-echo and pitch-catch techniques.

UGWs are increasingly becoming popular in the field of non-destructive evaluation and structural health monitoring [45]. The popularity is due to their ability to detect small flaws, moderate inspection ranges, and built-in transduction capabilities [46]. Advances in the understanding of UGWs have led to increased use in industry and the development of new applications for structural health monitoring. Guided wave inspection provides an efficient way to inspect large structures with only a few transducers, making it suitable for many types of structures [47].

In the field of Non-Destructive Evaluation (NDE) using guided waves, many types of transducers, such as wedge, comb, and electromagnetic acoustic transducers, are the most frequently used. Although these transducers are effective for maintenance inspections, there is a lack of research on testing their functionality on structures during operation, as required for in situ structural health monitoring (SHM). To address this issue, other transducers have been developed that are more lightweight, smaller in size, and cost-effective for in situ SHM. An example is the in-situ structural health monitoring technology studied using piezoelectric wafer active sensors (PWAS) guided waves for various inspection and health monitoring applications [48].

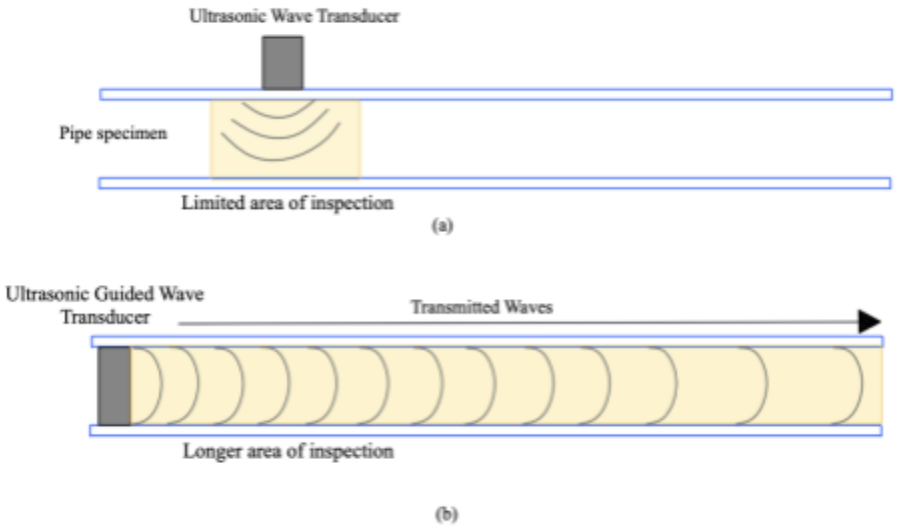

Figure 3. a) Limited area of inspection using UW method b) Longer area of inspection using UGWs method.

To improve the performance of UGWs in detecting and sizing defects, improvements in signal processing are required, especially in the extraction of features that can act as damage indicators [49]. The use of statistical features of ultrasonic signals, such as root mean square, variance, and kurtosis, has been successful in damage detection and can be extracted in either the time or frequency domains [50-51]. Macro Fiber Composites (MFCs) have proven to be a convenient and cost-effective solution as transducers for the generation of waves in scour rods [52]. These transducers are presented in the form of thin piezoelectric films and can be easily attached to the scour rod for the purpose of guided wave generation [53-55]. The compact size and low cost of MFCs make them an ideal option for in situ monitoring, as they can be unobtrusively attached to the scour rod without causing significant

weight or space penalties. The feasibility of using MFCs as transducers for scour rod wave generation is studied in this research.

2.2 Lamb Waves

Lamb waves, on the other hand, are a specific type of UGWs that propagate in thin plates or shells. They are named after the mathematician Horace Lamb, who first described them in 1917. Lamb waves are a type of wave that can occur in thin plate-like structures with parallel free boundaries. This phenomenon was first studied by Lowe [56], followed by an experimental study of guided waves and its material characterization by Chimenti [57]. Lamb waves are highly susceptible to interference from obstructions on their path, such as damage or boundaries. Despite this, they can travel long distances, even in materials with high attenuation ratios like carbon fiber-reinforced composites. This makes them useful for quickly examining a large area. Su *et al.* [58] has provided a more detailed understanding of the theory behind Lamb waves. The use of Lamb waves has been proven effective in detecting damage in thin plates [59-60]. Consider a thin plate with stress-free upper and lower surface with the total thickness of the plate is $2d$. The equation of motion for an isotropic elastic medium is given by Eq. 4:

$$\mu \nabla^2 u + (\lambda + \mu) \nabla\nabla \cdot u = \rho \frac{\partial^2 u}{\partial t^2} \quad (4)$$

where λ and μ are the Lamé constants and, ρ is the mass density and u is the displacement vector. Yu *et al.* [48] has a detailed outline and derivation of this equation. A Lamb mode can be either symmetric or antisymmetric, formulated by Eq. 5 - Eq. 8:

Symmetric modes $$\frac{tan(qh)}{tan(ph)} = -\frac{4k^2pq}{(q^2-k^2)^2} \quad (5)$$

Antisymmetric modes $$\frac{tan(qh)}{tan(ph)} = -\frac{(q^2-k^2)^2}{4k^2pq} \quad (6)$$

$$p = \sqrt{\left(\frac{\omega}{c_L}\right)^2 - k^2} \; ; k = \frac{\omega}{c_P} \quad (7)$$

$$q = \sqrt{\left(\frac{\omega}{c_T}\right)^2 - k^2} \; ; k = \frac{\omega}{c_P} \quad (8)$$

where h, k, c_L, c_T, c_p, and ω are the plate thickness, wave number, velocities of longitudinal and transverse modes, phase velocity, and wave circular frequency, respectively. When the wave equations are solved numerically using known material constants, the resulting dispersion curves provide valuable information about the material. Dispersion curves reveal the relationship between wave frequency and wave vector in the material, which can help analyze properties such as wave propagation speed and energy transfer. Additionally, dispersion curves enable determination of the group velocity of different types of waves in the material, which is crucial for understanding wave-matter interactions, energy transfer, and wave propagation phenomena.

Lamb waves have become an important research topic in NDE and SHM due to their ability to detect damage in structures without the need for physical access. The behavior of Lamb waves is highly dependent on the thickness, material properties, and geometric features

of the plate or shell, which makes them a useful tool for detecting defects such as cracks, delamination, and corrosion. Lamb waves exhibit two mode shapes, namely symmetric and asymmetric, throughout the plate. These modes are highly sensitive to changes in the material surrounding the plate, and the frequency-thickness product determines the type of mode shape and propagation velocity. The frequency depends on the input signal and plate thickness, and Lamb waves interact with the surrounding material on both sides of the plate structure. It's worth noting that an external constraint on the propagating material containing the Lamb wave could result in energy reflection due to a change in mechanical impedance at the site of the constraint.

Recent research has focused on developing advanced techniques for Lamb wave-based SHM. Piezoelectric devices are commonly used to introduce Lamb waves into a structure [61], but the use of MFCs has been proposed as an alternative method [62-63]. MFCs can introduce Lamb waves effectively, have high durability, and are easily bonded to the structure. To optimize damage detection, it is recommended to introduce only one Lamb wave mode, as this results in clear response signals without dispersion [47]. Low frequency Lamb waves are suitable for long range inspections, such as the detection of large scour holes, as they can propagate over longer distances. This study focuses on using Lamb waves for the detection of sediment levels on both surfaces of a thin plate, as they can indicate potential interactions with surrounding materials [64]. When an external constraint is applied to the material carrying the Lamb wave, a change in mechanical impedance can result in energy reflection at the constraint location. Therefore, in this study, Lamb waves generated by MFCs were explored as a sensing mechanism to evaluate soil-interfaces, with the end goal of monitoring scour.

Chapter 3. Analytical Procedures and Experimental Details

The purpose of this chapter is to provide a comprehensive discussion on the various aspects related to the validation of the piezoelectric sensor scour rod. It encompasses the hardware measurements, experimental setup details, and analytical procedures employed to ensure the functionality and reliability of the sensor system. In Section 3.1, the focus lies on the hardware measurement system utilized to generate Lamb Waves of specific frequencies and amplitudes. This system plays a crucial role in facilitating the excitation signals along the beam. Section 3.2 discusses the experimental details of the piezoelectric sensor scour strip. This strip is specifically designed to identify the locations of interest where local pressure changes occur. Section 3.3 introduces a new approach to investigate the response signals. It involves the utilization of cross-correlation analysis, which enables the determination of time lags of echoes in response signals. This analysis serves as a reliable method for precisely locating the location of interest. While the results are promising when the strip is placed horizontally, this setup does not fit well with the idea of burying the scour rod vertically into a sediment medium. To design a more robust scour rod, this study replaced the aluminum strip with an H-beam, which makes it easier to drive into the soil during on-site installation. The H-beam was buried in a sediment layer inside a tube, which can be used to mimic a driven scour rod for monitoring scour. Section 3.4 explains these details in greater depth. To track the progress of scour once the scour sensor is installed, a new feature extraction method was proposed that involves using the convolution of the input and output signals. This method is more viable when there are no clear echoes from the sediment layer's surface. Finally, Section 3.6 validates the first on-site installation of the proposed scour sensor rod under dry

conditions. This practical validation serves as a significant milestone in assessing the viability and applicability of the sensor system in real-world settings. Overall, this chapter explains the experimental validation towards building a versatile scour rod, the measurement system employed, and the techniques employed to collect and analyze the data towards a practical scour sensor prototype for real-world testing.

3.1 Measurements

The scour sensor system is in the form of a thin, slender aluminum strip that could be buried in soil for the purpose of measuring scour depth. This system consisted of two piezoelectric transducers, known as MFCs, bonded to the same end and face of the 1.8 m long strip using double-sided tape (Figure 4). As mentioned earlier in Section 2.2, the MFC can introduce Lamb waves effectively, have high durability, and are easily bonded to the structure. The two MFCs bonded to the rod are called as actuating MFC and sensing MFC. In order to generate lamb waves and record the responses after excitation, a hardware setup was used that included a waveform generator and an oscilloscope. The actuating MFC was connected to the waveform generator, while the sensing MFC was connected to an oscilloscope. Figure 5 illustrates the corresponding hardware setup. The primary purpose of an Agilent 33220A waveform generator was to generate suitable drive waveforms for the MFC actuator. This study uses first-order symmetric (S0) Lamb waves generated by MFCs in an UGWs sensing mechanism for the detection of soil-interfaces for scour monitoring purposes. This first-order symmetric wave in the form of a Gaussian sine wave pulse was outputted at a packet frequency of 2 kHz and an overall central frequency of approximately 22 kHz. The waveguide was generated by a waveform generator and transmitted through the actuator to the sensor

MFC. The multi-cycle Gaussian wave is a versatile and widely used signal in ultrasonic testing due to its ability to effectively propagate through solid materials and produce clear reflections, making it a suitable choice for scour detection applications. The Gaussian sine wave pulse utilized in this study is depicted in Figure 6. The central frequency was determined by adjusting the packet frequency in order to produce the largest reflected response. The electromagnetic pulse was generated with a burst and delay of 20 ms to allow sufficient time for the reflections from the previous pulse to dissipate. The sensing MFC was connected to a Keysight InfiniiVision DSOX3024T oscilloscope and the output waveform was averaged x50 to reduce noise in the acquired signals. The sampling rate for the oscilloscope was around 3.2 MHz, allowing high-resolution data acquisition. This setup, with the use of the MFCs and specified hardware, formed a pitch-catch configuration of monitoring. Figure 5 displays the hardware configuration utilized in this study. The actuator pulsed the wave packet intermittently, while the sensor received the first pass of the input pulse as well as a series of pulses reflected along the aluminum strip.

3.2 Aluminum Strip as a Scour Sensor Rod

As explained in Section 3.1, the scour sensor rod was in the form of a strip with two piezoelectric sensors mounted on the face of the strip. The actuator MFC excited the wave packet to travel along the length of the material and the reflections were collected back from the sensor MFC. These reflections are due to heavy impedance change such as difference in the local pressure or from the end of the strip. To simulate impedance change in the experiments, localized pressurized areas were introduced to the sensor strip using a buffered steel weight and distributed soil pressure. The scour strip sensor system was positioned

horizontally, and steel weights were positioned on the aluminum strip's top surface, which was also the surface where the MFCs were bonded, as shown in Figure 4. The weight used was 3.30 lbs and had circular cross-sectional base area. To ensure a consistent contact area, a buffer plate (washer) was employed. The weights were then positioned at 1 ft intervals from 1 to 5 ft. The sensor system described in Section 3.1 was used to create a scour measurement system, and tests were conducted to determine the location of the medium's interface. The response signals were recorded on an oscilloscope using a USB drive for data processing. The results presented by Funderburk *et al.* [37-38] confirmed that the combination of lamb waves and MFCs could be used to monitor local scour. However, the peak detect method used to determine the location of the interface presented certain challenges. False reflected responses could have a higher peak than the desired response, resulting in inaccurate results. Section 3.3 proposes an adaptation of an alternative method, called as time-of-flight method, that overcomes this issue and provides more accurate results. An experiment was conducted to evaluate the time-of-flight method using cross-correlation from the reflection of the S0 Lamb wave by a pressure interface that does not cause damage and to determine if the time-of-flight could be utilized to pinpoint the position of the applied pressure.

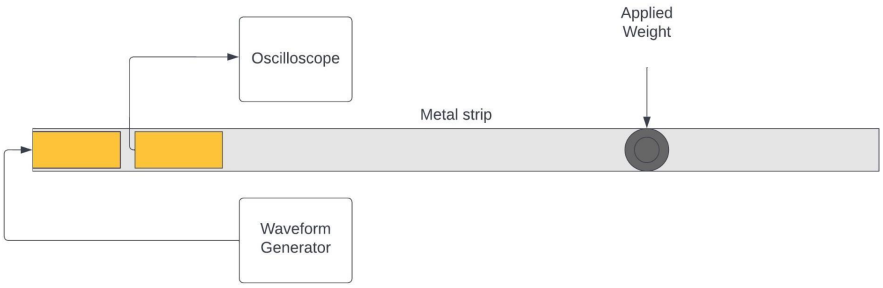

Figure 4. The figure presents a schematic representation of the experimental setup used in this study. The actuator MFC was connected to the Waveform Generator, and the sensing MFC was connected to an oscilloscope.

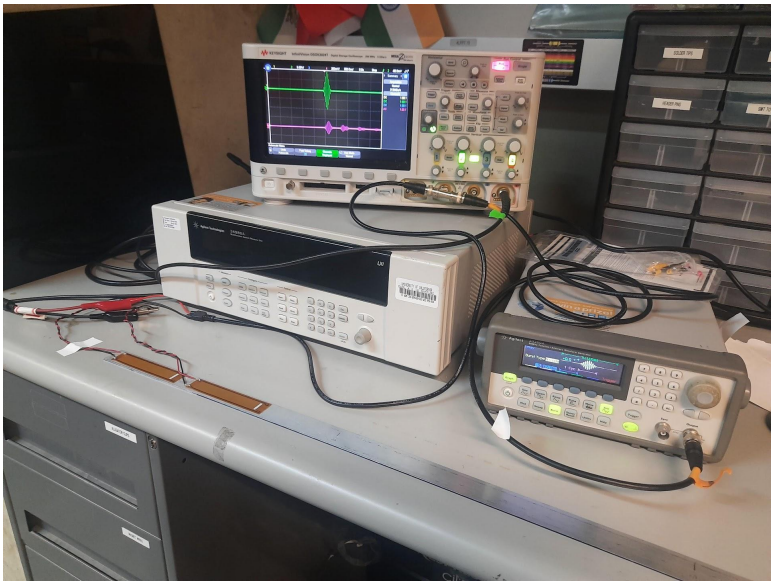

Figure 5. The figure depicts the experimental setup used in the study, with the MFC connected to the Waveform Generator and Oscilloscope. The metal strip was placed horizontally on a hard surface, and steel weights were applied at various locations to exert pressure.

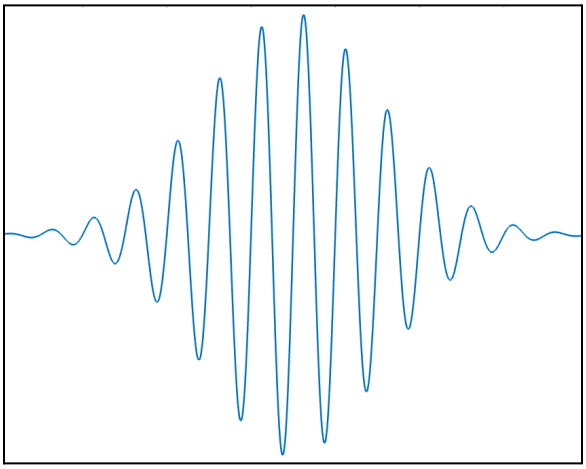

Figure 6. The figure displays the excitation signal utilized in the experiment, which is a multi-cycle Gaussian sine wave. This ultrasonic guide wave was generated by a waveform generator and transmitted through the actuator to the sensor MFC after reflections.

3.3 Evaluation of Time-of-Flight using Cross-Correlation Method

As explained in Section 2.1, the UGWs was a suitable method to study the impedance change along the structure. In this study, the ultrasonic pitch-catch method was used to locate the location of pressure change on a specimen. This method involves generating a short pulse of ultrasound using a transducer in contact with the specimen. The pulse travels through the material and reflects back to generate an echo signal in another transducer. By measuring the round-trip travel time of the signal, the distance traveled by the pulse and the speed of sound in the specimen can be determined. This approach is widely used for non-destructive testing and evaluation in various applications. During the experiment, a burst of UGWs was generated by the transducer and propagated down the metal rod. A portion of the pulse was reflected by the local pressure change interface, referred to as the pressure echo, while the remaining travels into the specimen, reflects off the opposite end, and returns to the transducer, known as the end-echo. A typical waveform with various echoes is shown in

Figure 7. Numerous other secondary echoes are present but are disregarded. By setting the time delay between the two bursts to avoid any overlaps of the reflections, the first two reflections were analyzed. A Gaussian ultrasonic burst is sent to the actuating MFC and serves as the excitation signal. This signal, illustrated in Figure 4, produced reflection echoes from the local pressure change along the way. The location of interest (L), that is the point at which there is a significant pressure change, can be calculated using travel time (t) of the ultrasonic burst and the velocity of the wave in the specimen used from the Eq. 9:

$$2L = v\,t \tag{9}$$

The velocity (v) of this wave is assumed as 5000 m/s [37-38]. To determine travel time with high accuracy, the cross-correlation method is adopted on the acquired signal. The cross-correlation of two arbitrary functions, *g(t)* and *h(t)* is defined in the Eq. 10:

$$Corr(g,h) = \int_{-\infty}^{\infty} g(\tau + t)\,h(\tau)\,d\tau \tag{10}$$

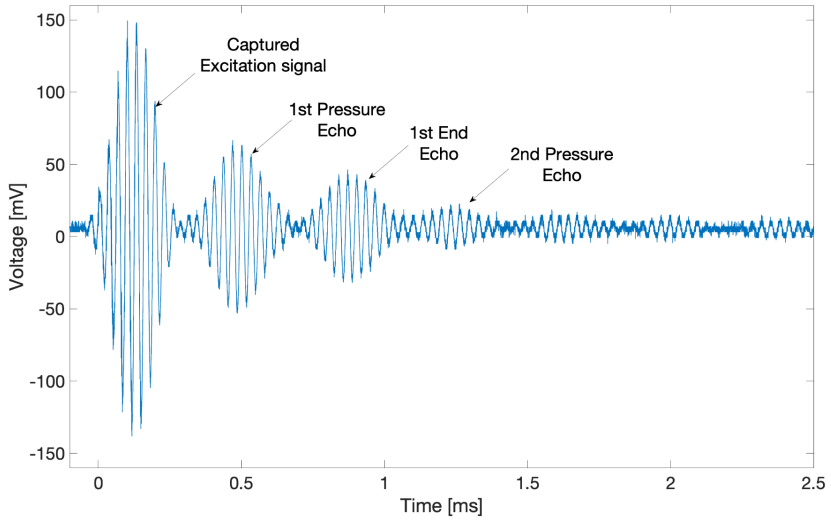

Figure 7. The figure illustrates the various echoes formed in the raw signal obtained from the sensor MFC, following the transmission of an excitation burst through the actuator.

3.4 Validation of the H-beam as a Scour Sensor Rod

The current method for detecting scour progress involves using a thin aluminum strip with a thickness of 0.2 mm. This strip can be buried in the soil bed attached to a support structure. However, if the scour sensor strip is attached to a support structure, there is a strong possibility of signals being severely damped since the thin plate is in direct contact with another material. Additionally, the strip is too thin and slender to withstand unforeseen difficulties during regular operations and in critical events occurring in the vicinity of hydraulic structures.

Considering these results, a proposal was put forward to replace the thin strip with an aluminum H-beam. The H-beam (Figure 8) can be driven directly into the soil bed and serve as a piezoelectric sensor rod, collecting data to predict scour processes. The use of the H-beam eliminates the damping effect on signals and provides more robust results. Additionally, the H-beam is less prone to buckling and other challenges during normal operating conditions. It also provides a more straightforward way to drive into the soil bed and can be braced against nearby structures to provide support. This approach is more effective for preventing scouring when compared to using thin, slender strips as support posts. The H-beam, denoted as "Architectural 6063 Aluminum H-Bars," was procured from McMaster.

The beam possesses a web thickness of 1/8 inch and a length of 6 feet. Its yield strength is noted as 16 ksi. It is important to note that the sensor configuration remains unchanged, and a pulse echo system can be achieved, as previously explained. The new H-beam setup appears to be a viable replacement for the current method. However, it was

necessary to conduct a thorough investigation of its functionality and ensure that it exhibits similar characteristics to the existing thin strip setup. To achieve this objective, an experiment was proposed to evaluate the performance of a new H-beam scour rod that replaces the metal strip with an aluminum H-beam. The experimental setup involved burying the beam vertically into a sediment medium at various depths to simulate real-world implementation scenarios. The schematic representation is depicted in Figure 9. The beam's length for the study is consistent with the previous section, i.e. 6 ft. The MFC connections will also remain the same as those of the previous section, but the excitation signal's amplification was necessary due to the limited voltage in the function generator. To address this issue, a Ciprian High Voltage Power Amplifier (HVPA) with an amplification factor of 200 times (x200) was utilized to increase the voltage from 9.5 V to 30 V peak-to-peak. The input wave was excited at 150 mV peak-to-peak voltage. This amplification was connected before the excitation signals were sent through the beam. Figure 9 shows the schematic flow of the connection using the amplifier. The higher signal energy was expected to generate at least two quality reflection echoes from the end of the beam for further analysis. To simulate scour, the experiment was conducted using a 5-inch outer diameter hollow acrylic clear round tube to bury the sensor-mounted H-beam, and sediment thickness was manually controlled. The sensing MFCs were positioned on the H-beam's web surface in a dry state. The sediment thickness was gradually increased in 1 ft. increments by adding quartz sands to the tank. For each sediment thickness increment, the corresponding response waveform was recorded for further analysis. The H-beam with MFC taped inside the tube is shown in Figure 10a. To examine the effectiveness of the current setup on various sediment types and to verify the viability of the feature extraction method in diverse media, an extended experiment was conducted following

the same procedures as described in this section. Three distinct sediment types were selected for the study: coarse sand, Ottawa F-65 (a silica-based sand), and regular soil. Figure 11 presents the three selected sediment types. All three sediment types were subjected to the same experimental procedures detailed in this section. Figure 10b shows the buried H-beam into the tube filled with 1 ft. of silica sand. A new feature extraction method was proposed for this updated setup. This method enables real-time monitoring and the development of an early warning system to ensure timely action is taken. This new approach was necessary as the reflected signals, once driven into the sediments vertically, did not produce intermediate echoes, unlike the earlier experiment described in Section 3.3. Since the time-of-flight method using cross-correlation is unsuitable in such scenarios, this new feature extraction method relies on other signal features, such as energy, convolution of input and response, to eliminate the need for intermediate echoes. Although it is evident that the signal characteristics are influenced by varying sediment types, this study does not focus on the impact of sediments on the feature extraction method.

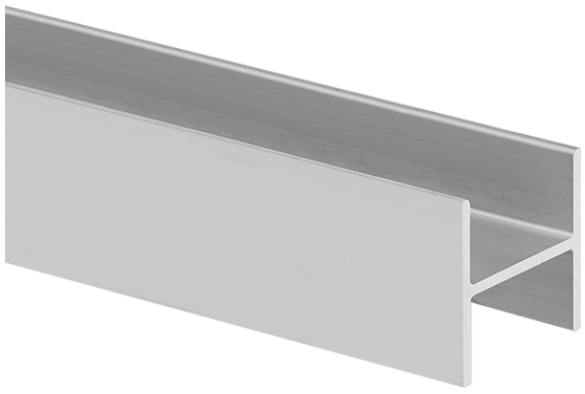

Figure 8. Three-dimensional (3-D) representation of the proposed aluminum H-beam, which is suggested to replace the previously proposed aluminum strip in this study.

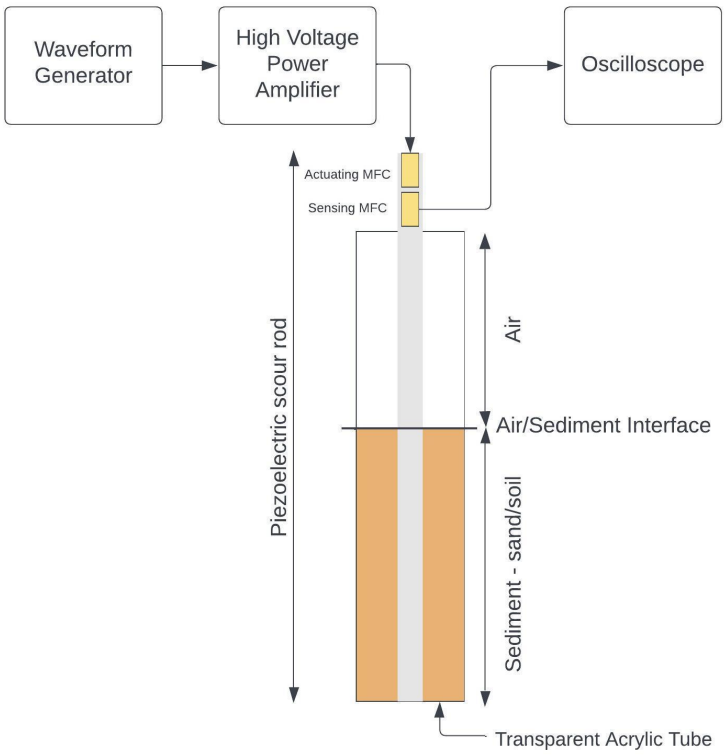

Figure 9. The figure illustrates a schematic representation of the laboratory setup used to validate the H-beam structure as a scour rod buried at different depths in sediments of varying thickness.

(a) (b)

Figure 10. a) The photo illustrates the MFCs mounted on the web of the H-beam structure inside a transparent acrylic tube. b) The photo shows the bottom of the H-beam structure buried in the Ottawa F-65 silica sand inside the tube. The sediment was used to evaluate the performance of the H-beam structure.

Figure 11. The figure displays the different sediments used in the study to validate the performance of the H-beam structure for different sediment types. The sediments include regular sand, Ottawa F-65 silica sand, and regular soil

3.5 Feature Extraction Method using Convolution

Convolution is a fundamental concept in signal processing that is widely used in various applications. In many real-world scenarios, signals are often generated by a system in response to an input signal, where the input signal is the excitation signal and the output signal is the response signal. The convolution operation is an essential tool in analyzing the relationship between an input and output signal because it allows us to extract information about the system's behavior. The mathematical equation for the convolution of two signals, $x(t)$ and $h(t)$, is given in Eq. (11):

$$y(t) = (x * h)(t) = \int_{-\infty}^{\infty} x(\tau)\, h(t-\tau)\, d\tau \quad (11)$$

where *y(t)* is the resulting convolution signal, * denotes the convolution operation. The function *h(t)* is the response signal of the system that is generated in response to the input signal *x(t)*.

In this study, the signal is referred to as the baseline signal when the strip/beam is not subjected to any external pressure. The baseline signal was obtained through a simple data acquisition experiment without any local pressure. The raw response signals that were acquired during the experiment, when the H-beam was buried at different depths of sediments, underwent several steps in the feature extraction method. Firstly, the response signals were filtered using a fourth-order Butterworth filter that bandpassed the frequency range from 20 kHz to 40 kHz. The Butterworth filter was essential in processing the received response signals, since the ultrasonic echo signal was likely to be mixed with noise of different frequencies. Butterworth analog transfer function transfer function magnitude is given by Eq. 12:

$$|H(j\omega)| = \frac{1}{\sqrt{1+\left(\frac{\omega}{\omega_c}\right)^{2n}}} \quad (12)$$

where ω_C is the cutoff frequency for nth order filter. The frequency range was determined from the fast Fourier transform analysis of the best response. The fourier transform of the time-domain signal, *f(t)* is defined by Eq. 13. Both the baseline signal and the response signals were filtered. Then, the convolution of signals took place between every

response signal and the excitation signal. A baseline convoluted signal was separately calculated by convoluting the baseline signal with its excitation signal. The residual convoluted signal was acquired by subtracting the baseline convoluted signal from the response convoluted signal. It had Gaussian-shaped echoes, and the most prominent echo among the rest was extracted as a separate signal. Root Mean Square (RMS) is the most important parameter that usually signifies the size and energy of the signal. For a digitized signal $x[n]$, the RMS is given by Eq. 14:

$$F(\omega) = \int_{-\infty}^{\infty} f(t)\, e^{-i\omega t} dt \tag{13}$$

$$RMS = \sqrt{\frac{1}{N} \sum_{n=0}^{N-1} (x[n])^2} \tag{14}$$

For the residual convoluted signal, this RMS value of an echo was used as the final feature to track the occurrence of scour. The idea is to keep a real-time track of this final feature and qualitatively assess the scour condition. The method also utilizes the relationship between the response and excitation signal, which was previously not incorporated. Additionally, since the excitation signal is the same throughout the monitoring process, evident changes in convolution signals are observed as response signals change. This newly proposed feature extraction method is validated through a set of experiments explained in the previous section.

3.6 Pilot Testing On-Site Installation

The transition from a laboratory prototype to a real-world application in structural health monitoring poses a significant challenge that requires careful planning and consideration of various factors. Safety, ease of installation, and protection from environmental conditions are critical factors that must be taken into account. One approach to addressing these challenges is to brace the newly designed H-beam piezoelectric to the bridge pier where scour progression needs to be monitored. As shown in Figure 12, this approach involves obtaining data related to scour monitoring using a specially designed setup. To test and validate this idea without the need of bracing the beam, an experimental setup was proposed in a field setting under dry conditions. The Englekirk Structural Engineering Center was selected as the site of investigation, and following a visual inspection, the soil condition at the center was identified as clay. However, the top layer of the site was covered with loose soil, while the soil below 2 inches was denser than that used in the lab setup for burying the scour beam. As a result, burying the beam at various depths proved to be a challenging task. To overcome this difficulty, a Minuteman XL8 Gas Post Driver (Figure 13) was utilized to facilitate the beam driving process. All safety protocols were meticulously adhered to in order to prevent any damage to the beam or injury to the personnel involved. The machine operates on regular gasoline, and the beam was properly inserted into the metal chuck of the driver, lifted along the beam, and placed at the desired location on the site (Figure 14a). Once the beam was accurately positioned, the driver was started, and the beam was driven into different depths for data acquisition, consistent with the MFC connection method outlined in Section 3.1

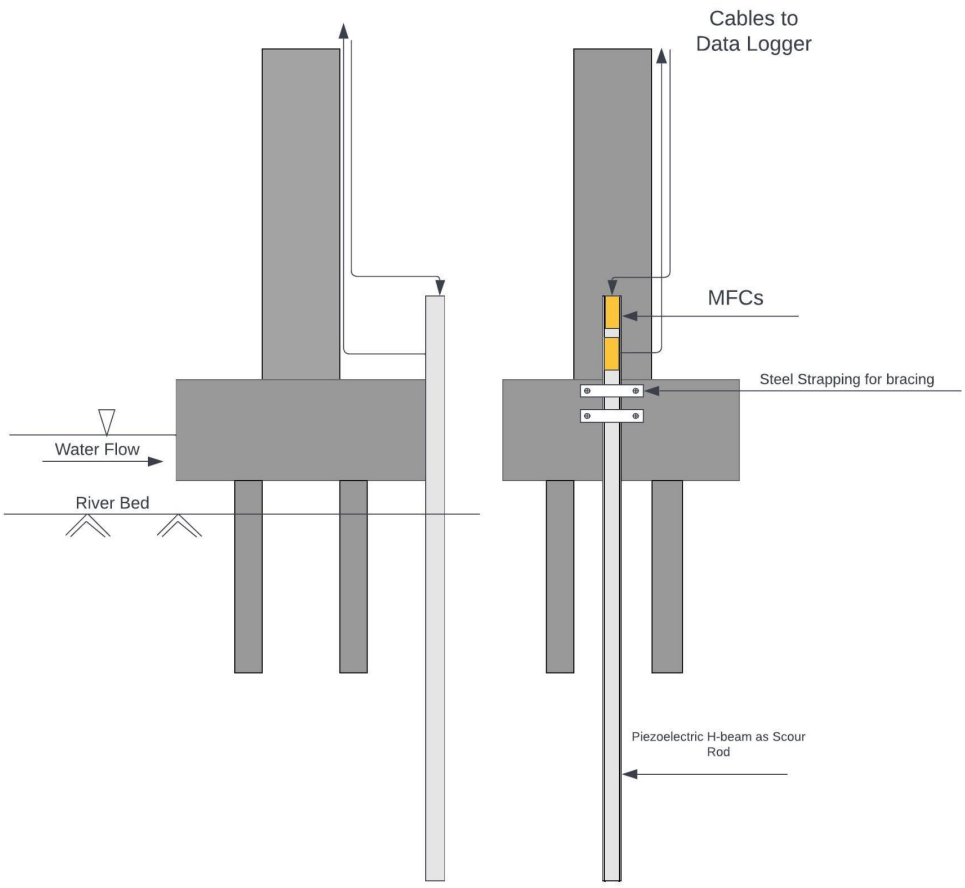

Figure 12. The figure presents a schematic representation of a future deployable H-beam scour rod into the riverbed, with sensors mounted and braced to a support, and connected to a data acquisition unit. The setup is shown from both front and side views, highlighting the positioning of the H-beam system and the sensors for detecting scour in real-world environments.

Figure 13. The Minuteman XL8 Post driver, which is intended to drive the H-beam into the ground during on-site installation.

(a) (b)

Figure 14. a) The figure shows the actual site for beam driving, which consists of a dry soil top layer and clayey soil underneath b) The H-beam was driven into this site, and MFCs were mounted on it.

To ensure that the sensors remained undamaged, the MFCs were removed from the surface of the beam every time the beam had to be driven. Once the desired depth was attained, the sensors were repositioned to acquire data (Figure 14b). This process was carried out multiple times to obtain data at various depths. The beam was driven in increments of 4 inches until a depth of 24 inches was reached for this study. This was done to ensure that the feature extraction method could discern between different depths and confirm the validity of

the new setup in a real-world test case. Electrical connections were also carried out on site, laying all the necessary equipment nearby to the installed beam as shown in Figure 15. This installation process necessitates the presence of at least two individuals equipped with personal protective equipment and an overseer to ensure safety.

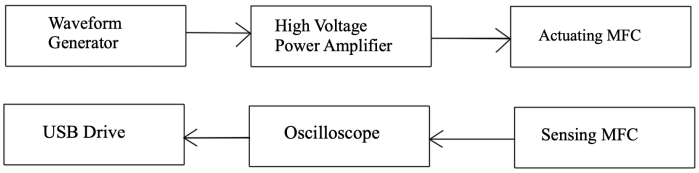

(a)

(b)

Figure 15. The figure depicts the on-site hardware setup used in the study, including a waveform generator, oscilloscope, and high-voltage amplifier a) Schematic representation of the hardware connection. b) On-site hardware connection.

Chapter 4. Results and Discussion

Chapter 3 of this experimental study described the progression from using an aluminum strip to employing a H-beam, as well as from conducting laboratory conditions to performing a field test on a dry soil site for the installation of the sensor scour rod. Initially, the aluminum strip was laid horizontally on a hard surface with weights placed on it to identify the location of interest. The location was determined by cross-correlating different echoes. However, due to its limitations, the aluminum strip was replaced by a H-beam. The H-beam was subsequently buried at varying depths in a transparent tube to validate the feature extraction method outlined in Section 3.5. Finally, the H-beam setup underwent testing on a dry conditioned clay site to facilitate the driving process for a future installation. This chapter discusses the results obtained from the aforementioned progression towards developing a robust prototype of the scour sensor rod.

4.1 Time-of-Flight Method using Cross-Correlation Results

In this thesis, the cross-correlation was performed between the signal containing information related to the pressure difference (pressure-echo) and the end of the strip (end-echo). To make it easier to understand, the first signal of interest includes both a pressure echo and an end echo, while the second signal of interest only includes an end echo. These signals can be seen in Figure 16. In order to analyze the signals, a particular interval containing information from both the first and second signals of interest was duplicated, and then a cross-correlation was performed between the signals. It's worth noting that it is not essential to select the window perfectly for the duplicated signal. It can be seen in Figure 17 that after cross correlation both signals, pressure-echo and end echo, show a Gaussian-like

profile. Once the peaks are known of this profile, it was easy to determine the time delay between the maxima of the central peaks. The approach was applied to different location depths to acquire the location of interest. Figure 18 shows the measured values of the location of interest where the steel weights were applied. The average percentage of error over the five measurements was found to be roughly 7%. It should be noted that this method is best suitable when the intermediate echos, similar to the pressure echos, are generated by the guided waves along their travel on the material. The approach is more deterministic and precise in comparison to the method that was proposed earlier using only peak detection of the response signal.

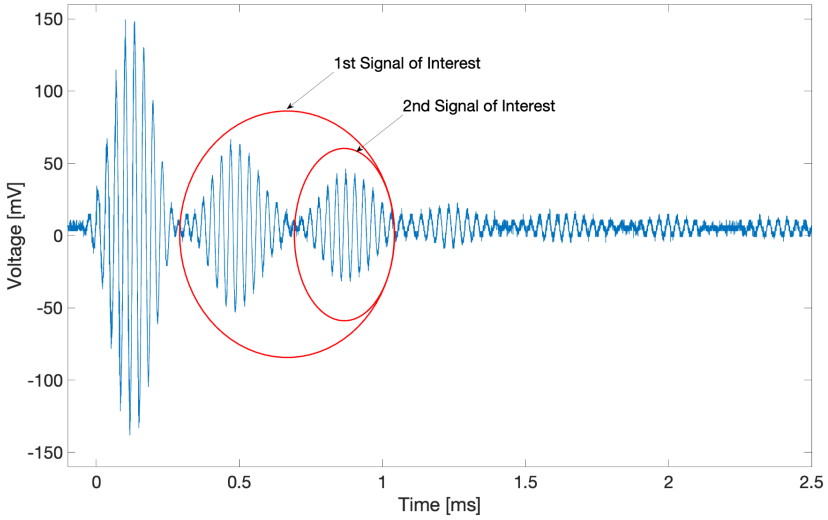

Figure 16. The figure demonstrates the two signals of interest that were selected for cross-correlation to estimate the time of flight. The first signal of interest encompasses both the pressure echo and the end echo, while the second signal of interest only encompasses the end echo. The time of flight was estimated by calculating the delay between the two signals of interest through cross-correlation analysis.

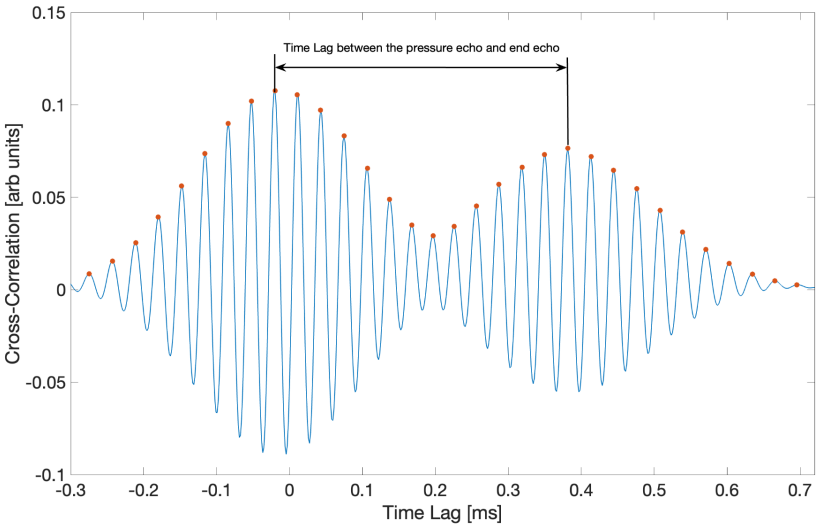

Figure 17. The figure shows the cross-correlation results for the first and second signal of interest for a typical measurement of delay between the pressure and end echo.

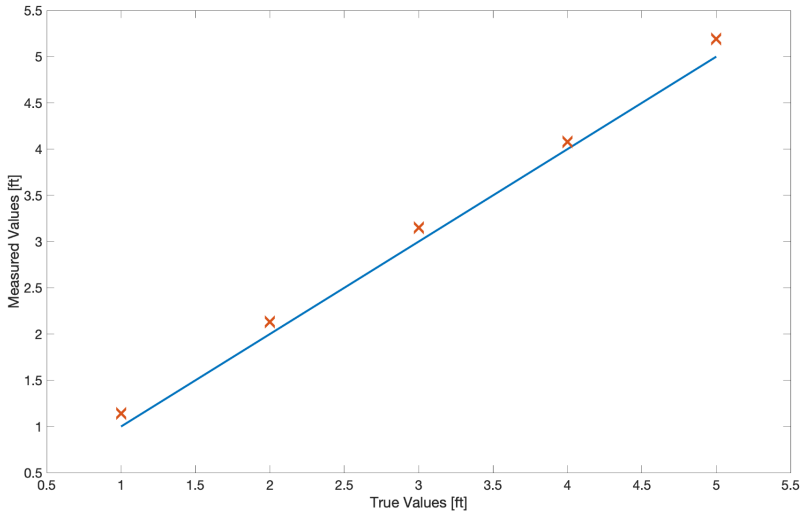

Figure 18. Cross-correlation results for the measured values of the location of the weight applied versus the true location, using the time-of-flight method.The results demonstrate that the time-of-flight method works well to provide a better estimate of the location of the weight applied compared to the measured values obtained directly from the sensor data.

4.2 Results for H-beam as Scour Rod with Feature Extraction Method

Figure 19 illustrates a comparison of the signals, specifically the first reflected echo, obtained from utilizing a thin strip and an H-beam in the aforementioned application for better comprehension. The similarity between the acquired signals is apparent, albeit the peak voltages vary due to the difference in the cross-section of the beam and the strip (Figure 20). Nevertheless, it can be observed that the H-beam was a suitable substitute. The raw signals obtained by burying the H-beam at different depths in regular sand are plotted against the y-axis Voltage in Figure 21.

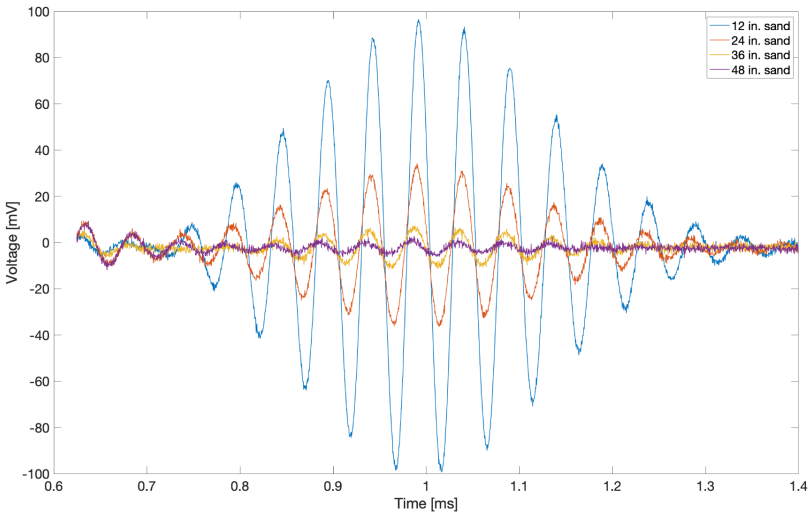

(a)

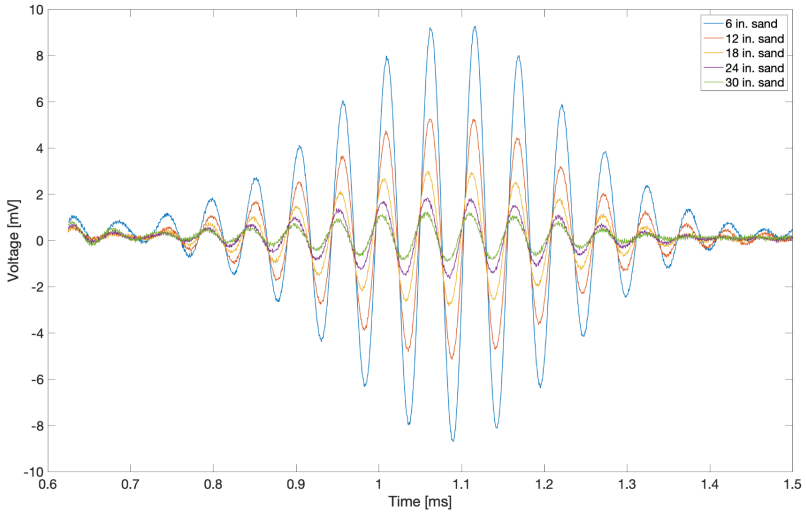

(b)

Figure 19. Comparison of the reflected echoes from a) an Aluminum thin strip and b) an Aluminum H-beam, both used as scour rods. While the pattern of reflection remains the same, the magnitude of the reflected voltage is different.

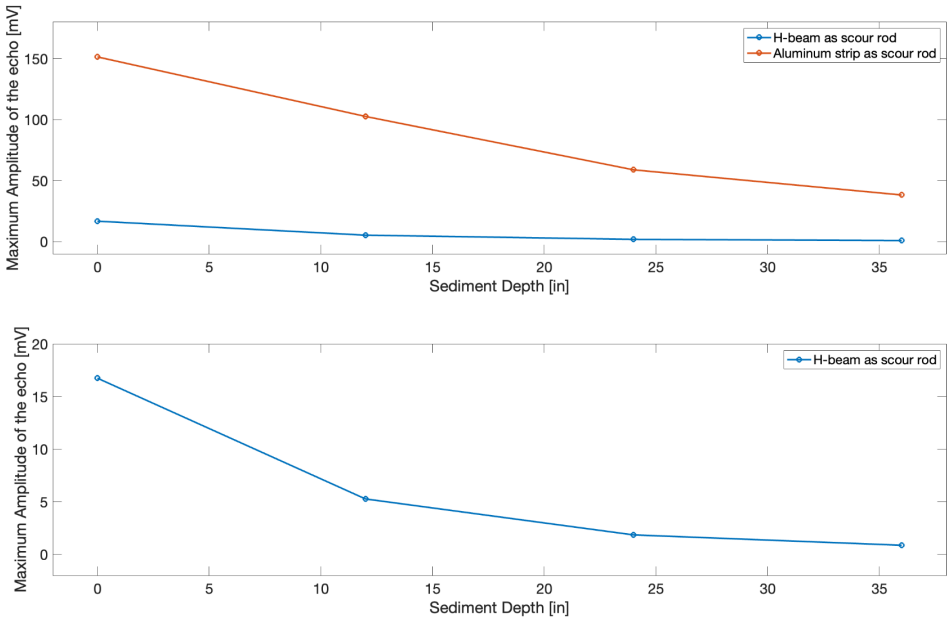

Figure 20. Comparison of the maximum amplitude of the reflected echoes from a) an Aluminum thin strip and b) an Aluminum H-beam, both used as scour rods. The peak voltage is dropped by 10 times when an H-beam is used instead of the aluminum strip.

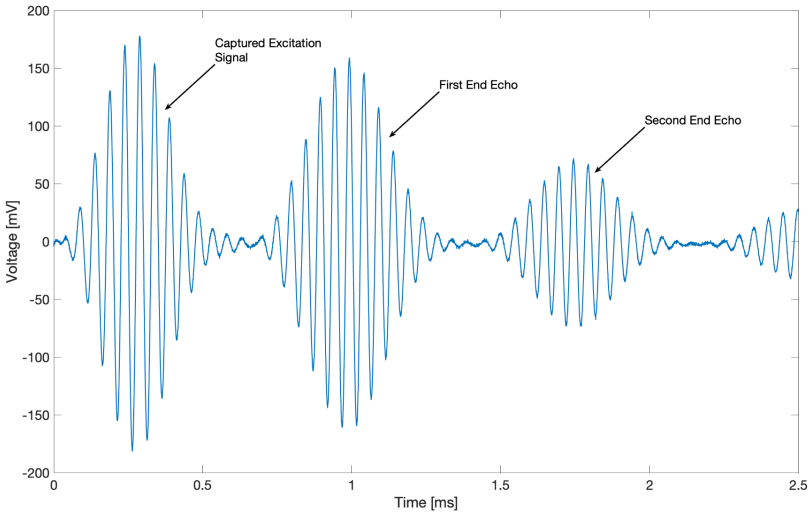

Figure 21. Figure showing a typical response signal from the sensing MFC mounted on the H-beam. No intermediate echo observed in the response signal due to sediment interface, precluding the use of time-of-flight method.

While examining the figure, it becomes apparent that there are no intermediate echoes that can be utilized to determine the location interface through the time-of-flight method discussed earlier. Nevertheless, a noticeable distinction is the dissimilarities in the peak voltages of the acquired signals.. This indicates that UGWs are sensitive to changes in the sediment depth.

The response signals that were obtained underwent the feature extraction method, as explained in Section 3.5, to obtain residual convoluted signals. It is intriguing to observe that the fast fourier transform (FFT) of the filtered echo displays varying magnitudes at different depths, while maintaining a central frequency of approximately 20.76 kHz as shown in Figure 22. It is important to note that a multi-cycle Gaussian wave was used as the excitation signal

in this study, as depicted in Figure 6. The same experimental setup was conducted over three different sediments to ensure that the feature extraction method is capable of showing feature change regardless of the sediment it is driven into. Figure 23 shows the convoluted signals of the response signals for the different sediments that were subjected to different depths of sediments, for a fair comparison. It can be seen that there were small variable changes in the voltage magnitudes, but the signals showed the same trend as those of the other sediments. The baseline convoluted signal was subtracted from these response convolution signals to obtain the residual convoluted signals. The first echo from the interval, as shown in Figure 22, was separated to calculate the Root Mean Square (RMS) of the echo as a feature. This feature has the potential to track every burst's response feature that was sent out from the MFCs and provide real-time qualitative analysis of the local scour where the beam would be driven. The bar graph in Figure 24 displays the RMS values of the residual convoluted signal's echo for various sediment depths. The RMS value reduces as the depth of the scour increases, indicating the potential of using the RMS feature to determine the scour depth with 30% as the proposed control line for inspection.An experiment was conducted to examine the sensitivity of a specific feature to smaller sediment depths. Regular sand was used, and the sediment depths were increased by only 6 inches for each increment. The Gaussian signal was excited with a peak-to-peak voltage of 6 V and amplified by a factor of 5 to reach 30 V peak-to-peak, as previously described. The experiment was repeated five times to gather statistical data and ensure the reliability of the feature. The convoluted signals obtained from one of the experiments were analyzed to determine the echo, and the results are depicted in Figure 25. The RMS values of the residual convoluted signal's echo were calculated for different sediment depths. These values, along with their associated error bars representing

variability, are shown in Figure 26. The confidence bounds were included to assess the standard deviation of the RMS values from the echo. It should be noted that due to the variation in excitation voltage compared to the earlier experiment, the peak RMS values in this experiment are slightly higher. However, the overall results align with those obtained from the previous experiment. The analysis of the data revealed that the aforementioned feature exhibits a high sensitivity to even minor changes in scour depths. Moreover, the feature demonstrated robustness in assessing the progress of scour, as confirmed by the consistent results obtained throughout the experiment. However, for precise quantification of the depth, a polynomial regression can be utilized. The calibration of the river bed's soil is necessary before implementing the scour monitoring process to determine scour's depth since the feature is dependent on the type of sediment.

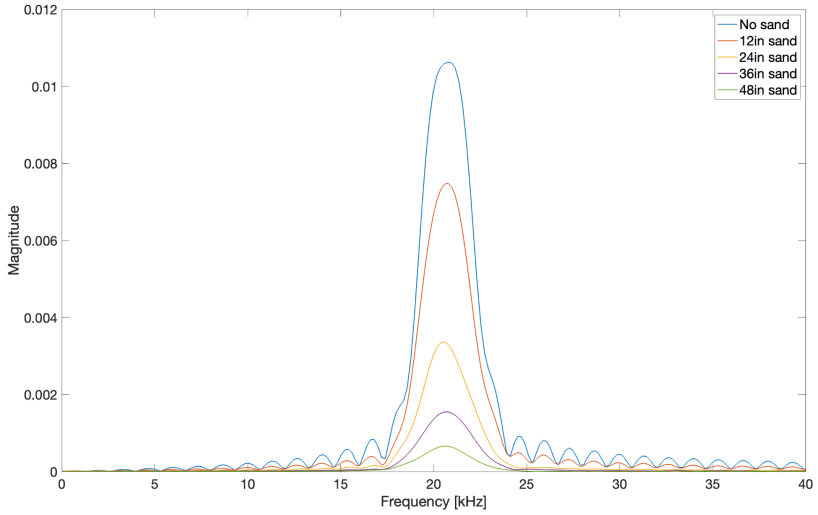

Figure 22. Fast Fourier Transform (FFT) of the reflected echo from the H-beam scour experiment for different depths of regular sand, showing consistent frequency but varying magnitudes.

Figure 23. Convoluted signals for different depths in three types of sediments - a) regular soil, b) regular sand, and c) Ottawa F-65 silica sand.

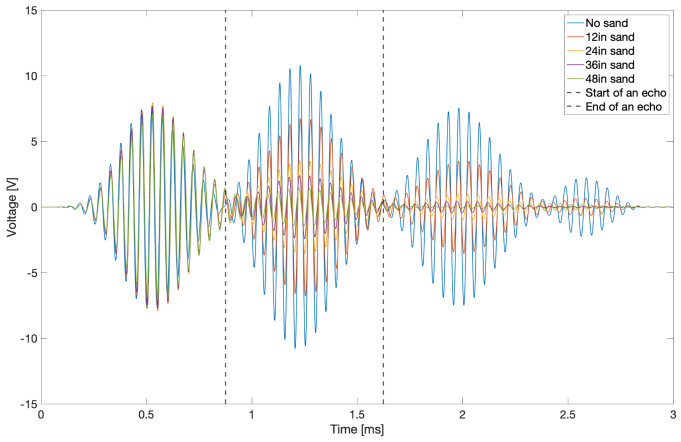
No sand
12in sand
24in sand
36in sand
48in sand
Start of an echo
End of an echo
Voltage [V]
Time [ms]

(a)

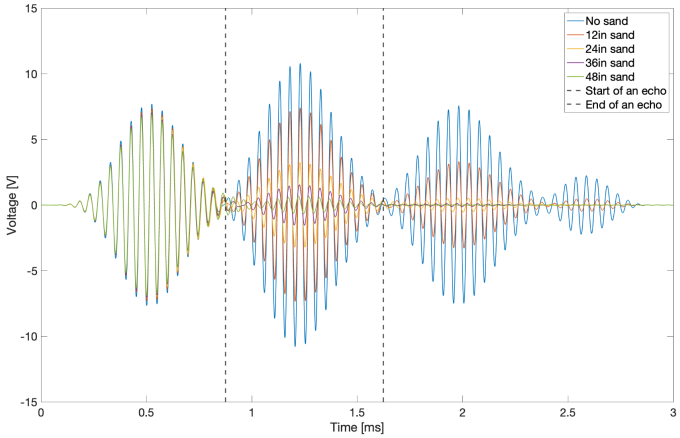
No sand
12in sand
24in sand
36in sand
48in sand
Start of an echo
End of an echo
Voltage [V]
Time [ms]

(b)

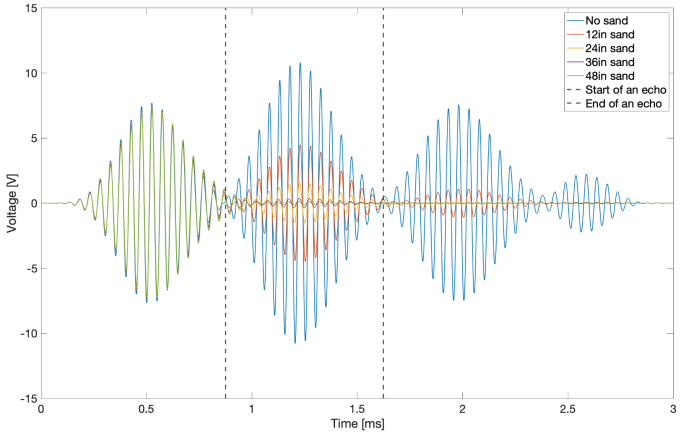
No sand
12in sand
24in sand
36in sand
48in sand
Start of an echo
End of an echo
Voltage [V]
Time [ms]

(c)

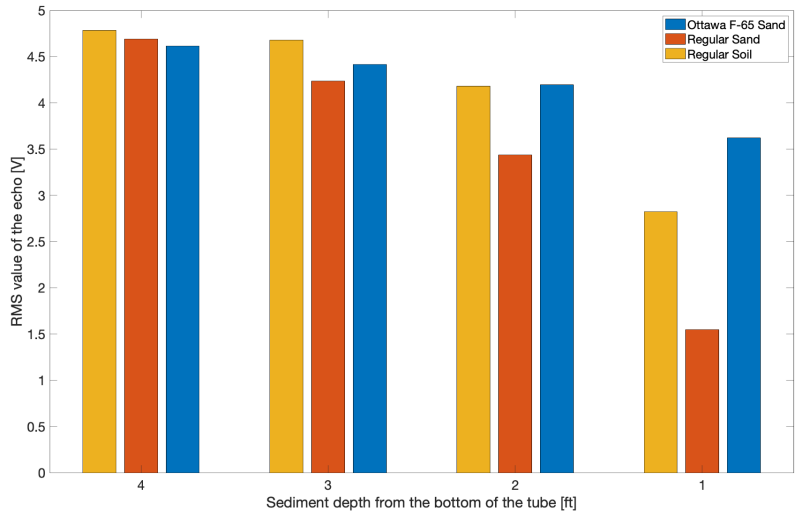

Figure 24. Comparison of different sediment types at various depths when the H-beam was buried in the tube. RMS values decrease as depth decreases for all sediment types. Note that the same amount of sediment in the tube yields a close RMS value, indicating that the method is versatile irrespective of the medium.

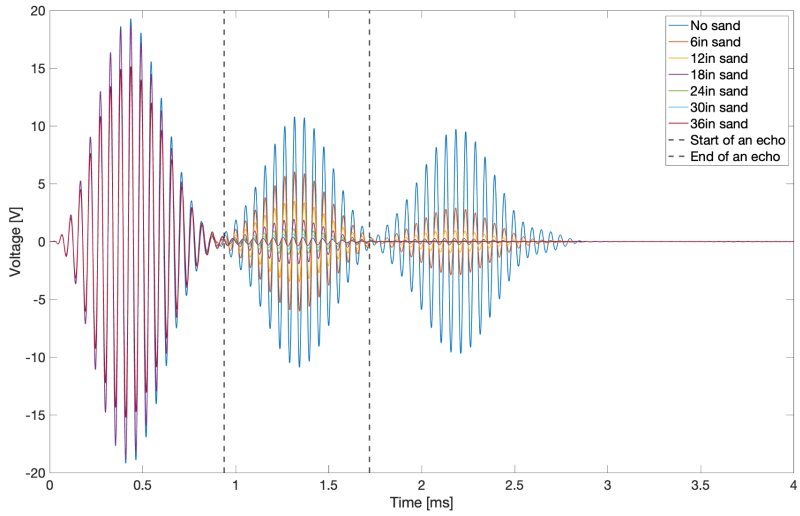

Figure 25. Convoluted signals for the regular sand with an increment of 6 in. of sediment depth in the tube.

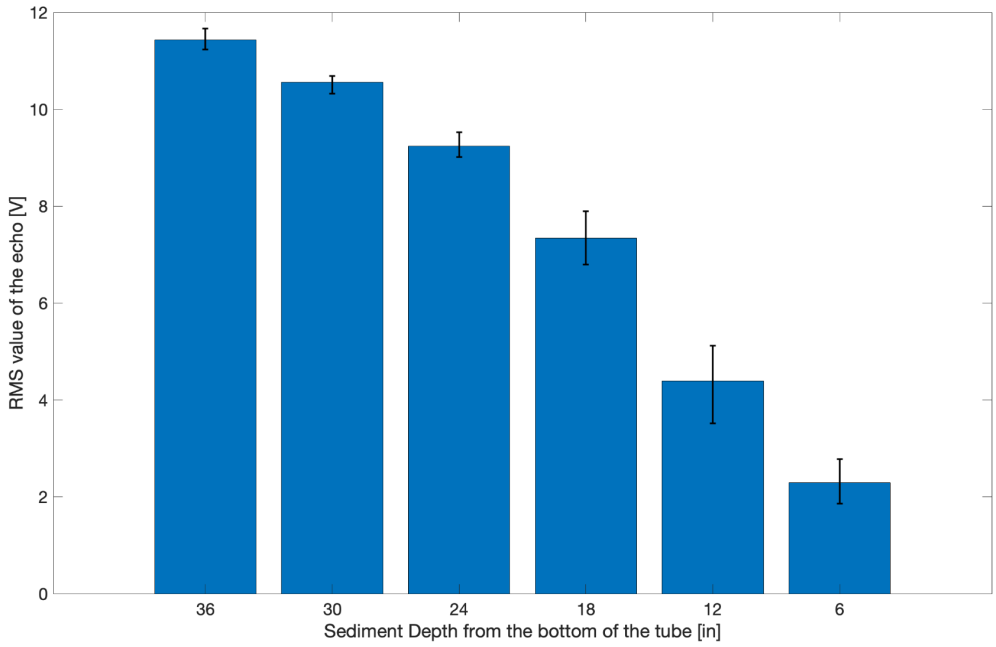

Figure 26. RMS values decrease as depth decreases for the regular soil along with the error bars. The feature adopted was able to identify smaller changes in the scour depth.

4.3 On-site Installation Results and Discussion

Figure 27a shows an image of two personnel using a post driver to drive the H-beam into the dry soil site. In Figure 27b, the installed beams at two different depths on the site are depicted. During the installation process at the site, a major observation was made regarding the non-uniform density of the soil as the beam was being driven. This inconsistency in density may have resulted in the damping of the response signals. It is worth noting that the laboratory conditions used a uniform and dense sand medium. Despite this, the data obtained from the on-site setup was processed using the same feature extraction method as explained in Section 3.5 to ensure consistency with the laboratory results. RMS values were obtained from the echo and plotted for analysis. It was observed that the results were consistent with the

expected outcomes (Figure 28), even when the soil density beneath the beam changed. It can be said that this feature is able to identify change for different depths of sediment, in accordance with that of laboratory results. However, the signals were heavily damped after only 1 foot of driving into the ground, which could pose a challenge in retaining echoes from beams that are driven to greater depths. Furthermore, the system's installation in wet conditions may pose significant challenges since it was not tested in this study. One of the difficulties encountered involves ensuring a secure hardware-to-sensor rod connection, given that the delicate wiring is susceptible to environmental conditions. Additionally, protecting the system from unexpected events that may cause damage is essential. Therefore, it is crucial to have a plan in place to safeguard the system and monitor its functionality in real-time and that is where bracing the H-beam to the support with steel strapping can be beneficial. On the brighter side, the installation setup is a straightforward process with successful implementation alongside validation of the feature extraction method. The total hardware and signal processing integration of the scour system can provide an effective and cost-efficient solution compared to other commercial options available in the market.

(a) (b)

Figure 27. (a) Manual driving of the H-beam using the minuteman X Post driver and (b) two H-beams hard driven into the on-site clay soil, demonstrating the ease and straightforwardness of the driving process.

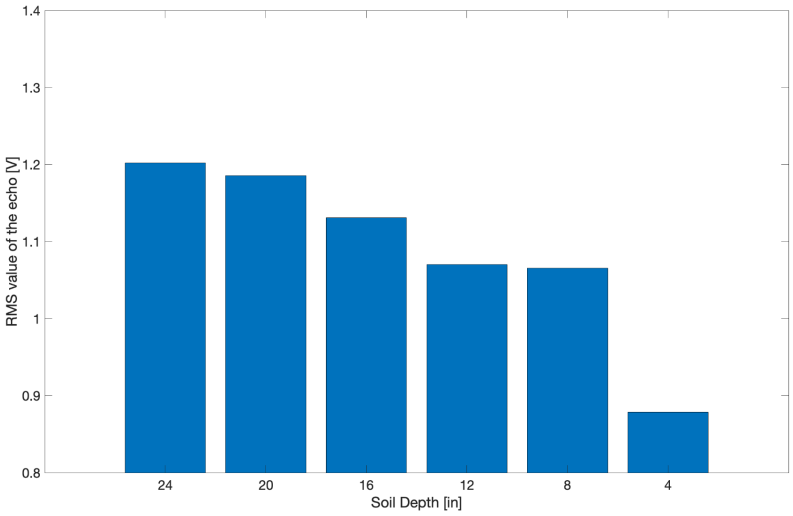

Figure 28. A decreasing trend in the RMS values for H-beam driven on-site at different depths. This trend highlights the potential to monitor the scour progression in real-time by tracking the changes in RMS values.

Chapter 5. Conclusions

Local scour has garnered a lot of attention in particular because of its disastrous effects on public safety and socioeconomic prosperity. UGWs are an emerging sensing technique based on which a potential scour monitoring system can be developed. The objective of this study was to design a more robust scour rod that is feasible and viable in terms of deployment and develop data processing techniques that are capable of identifying the changes in the sediment's depth. The proposed piezoelectric rod consists of an aluminum H-beam coupled with two piezoelectric sensors, called as MFC, which act as a pitch-catch data acquisition using the UGWs. A new method using convolution of the excitation and response signals was proposed to extract the feature that corresponds to the changes in the sediment's depth in order to enable real-time monitoring of scour. This feature has the capability to produce the real-time assessment of the scour progress. The functionality of the piezoelectric sensors for actively monitoring local scour at bridge piers was successfully validated through experiments. The newly designed H-beam piezoelectric scour sensor rod was found to be a promising upgrade from previous prototypes. The robust design of the H-beam as a scour rod and feature extraction method was able to detect changes in soil interface along the length of the beam, whether due to scour or deposition. A practical implementation of the design was also carried out in a field test and validated its capabilities alongside a smooth installation process as a scour monitoring system.

However, the exploration of deconvolution as a complementary analysis technique can be considered for enhancing the experimental findings. Deconvolution is a mathematical operation that aims to reverse the effects of convolution, thus enabling the separation of

signals that have been combined. Unlike convolution, where the response signals are convolved with the excitation signal, deconvolution involves dividing the Fourier Transforms of the response and excitation signals. This division compensates for any potential variations in the excitations and provides a more accurate representation of the "net" response of the beam as it interacts with different levels of scour. By incorporating deconvolution in the analysis, the amplitude of the net response can be directly assessed, circumventing the need for indirect measurements obtained through convolution. This approach also holds the potential to enhance the sensitivity and accuracy of scour monitoring, particularly in cases where the excitation signal varies over time or between experiments. While the present study successfully employed convolution due to the constancy of the excitation signal, deconvolution can be highly valuable for future investigations. Thus, the deconvolution of excited signals and response signals will be thoroughly explored as a continuation to this study.

The future plans for the piezoelectric scour sensing system entail its ployment in real-testing conditions to monitor the progress of local scour. While the proposed feature extraction method shows promise, there is a need to address the computational costs and memory storage requirements associated with the method. Time complexity of an algorithm refers to the computational efficiency or performance, describing the amount of time it takes to run as a function of the input size. It measures how the algorithm's execution time increases with the growth of the input. Currently, for the proposed method each convolution iteration has a time complexity of $O(n^4)$, which can be computationally intensive and high memory cost if data is collected frequently and stores all the information. To mitigate this, a solution is to extract and store only the essential feature, RMS value of the residual convoluted echo,

thereby optimizing computational costs and memory requirements. Additionally, there is a plan to develop a new data acquisition unit that combines the functions of a wave generator and oscilloscope. This integrated hardware will not only facilitate the excitation of the actuator but also enable the collection and processing of reflected waves. Moreover, investigating the amplification of signals from the sensor MFC before acquisition is of interest. This could potentially improve the quality of signals for the first and second reflections, as damping typically affects most reflections. It would also be interesting to analytically derive the baseline response signal using the material's dispersion curve and its properties. This can be used as reference and thus any attenuation due to scour depth change can be investigated Furthermore, a generalized scour estimation approach can be developed by leveraging the accumulated data over time. Machine learning techniques, such as transfer learning, can be employed to create a versatile model that can adapt to different locations. This real-time scour monitoring information will enable bridge inspectors to make informed decisions regarding the need for further investigation. Therefore, continuous research and refinement of these techniques are necessary to achieve this objective and ensure the ongoing improvement of water resource infrastructures.

References

[1] U.S. Geological Survey, Department of the Interior/USGS

[2] Melville, B. W. (1975). Local Scour at Bridge Sites. (Doctoral dissertation). University of Auckland, School of Engineering.

[3] Arneson, L. A., Zevenbergen, L. W., Lagasse, P. F., & Clopper, P. E. (2012). Evaluating Scour at Bridges. HEC-18. Fifth Edition, Hydraulic Engineering Circular No. 18. Publication No. FHWA-HIF-12-003. U.S. Dep. Transp. Fed. Highw. Adm., (18), 340.

[4] American Association of State Highway and Transportation Officials. (2010). AASHTO LRFD Bridge Design Specifications.

[5] Shirole, A. M., & Holt, R. C. (1984). Planning for a Comprehensive Bridge Safety Assurance Program. Transport Research Record, vol. N991, Washington DC, Transport Research Board, 137-142.

[6] Wardhana, K., & Hadipriono, F. C. (2003). Performance of Bridge Expansion Joints. Journal of Performance of Constructed Facilities, 17(3), 144-150.

[7] Kamojjala, S., Gattu, N. P., Parola, A. C., & Hagerty, D. J. (1994). Analysis of 1993 Upper Mississippi Flood Highway Infrastructure Damage. Proceedings of the 1st International Conference of Water Resource Engineering, American Society of Civil Engineers, New York, pp. 1061-1065.

[8] Neumann, J. E., Price, J., Chinowsky, P., Wright, L., Ludwig, L., Streeter, R., Jones, R., Smith, J. B., Perkins, W., Jantarasami, L., Martinich, J. (2015). Climate Change Risks to US Infrastructure: Impacts on Roads, Bridges, Coastal Development, and Urban Drainage. Climatic Change, 131(1), 97-109.

[9] Mueller, D. S., & Wagner, C. R. (2005). Field Observation and Evaluations of Streambed Scour at Bridges. FHWA, Louisville, KY, May.

[10] Richardson, E. V., & Richardson, J. R. (1989). Bridge Scour. University of Colorado, Boulder, CO.

[11] Browne, T. M., Collins, T. J., Garlich, M. J., & O'Leary, J. E. (2010). FHWA-NHI-10-027: Underwater Bridge Inspection.

[12] Briaud, J. L., Ting, F. C. K., Chen, H. C., Cao, Y., Han, S. W., & Kwak, K. W. (2001). Erosion Function Apparatus for Scour Rate Predictions. Vol. 5, No. February, 105-113.

[13] Prendergast, L. J., & Gavin, K. (2014). A review of bridge scour monitoring techniques. Journal of Rock Mechanics and Geotechnical Engineering, 6, 138-149.

[14] Huang, L., Wang, D., & Zhou, Z. (2007). A New Type of Optical FBG-based Scour Monitoring Sensor. Pacific Science Review, 9(1), 103-109.

[15] Chen, H., Michalis, P., & Valyrakis, M. (2020). Additive Manufacturing of Electrical Strain Gauges for the Monitoring of Embankment Failures.

[16] Lin, Y. B., Chang, K. C., Lai, J. S., & Wu, I. W. (2004). Applications of Optical Fiber Sensor on Local Scour Monitoring. Sensors, 2004 IEEE, Vienna, Austria, 832-835 vol.2.

[17] Liu, W., Zhou, W., & Li, H. (2022). Bridge scour estimation using unconstrained distributed fiber optic sensors. Journal of Civil Structural Health Monitoring, 12, 775-784.

[18] Bao, T., & Liu, Z. (2016). Vibration-based bridge scour detection: A review. Structural Control and Health Monitoring, 24(7).

[19] Dahal, P., Peng, D., Yang, Y., & Sharif, H. (2013). RSS based bridge scour measurement using underwater acoustic sensor networks. Communications and Network, 5, 641-648.

[20] Lin, Y. B., Lai, J. S., Chang, K., & Li, L. S. (2006). Flood scour monitoring system using fiber Bragg grating sensors. Smart Materials and Structures, 15, 1950.

[21] Anderson, N. L., Ismael, A. M., & Thitimakorn, T. (2007). Ground-Penetrating Radar: A Tool for Monitoring Bridge Scour. Environmental & Engineering Geoscience, 13(1), 1-10.

[22] Raju, R. D., Nagaranjan, S., Arockiasamy, M., & Castillo, S. (2022). Feasibility of using green laser in monitoring local scour around bridge pier. Geomatics, 2(3), 355-369.

[23] Yao, C., Darby, C., Hurlebaus, S., Price, G. R., Sharma, H., Hunt, B. E., Yu, O. Y., Chang, K. A., & Briaud, J. L. (2010). Scour monitoring development for two bridges in Texas. Geotechnical Special Publication, no. 210 GSP, 958-967.

[24] Richardson, J. R., Price, G. R., Richardson, E. V., & Lagasse, P. F. (1996). Modular magnetic scour monitoring device and method for using the same. U.S. Patent No. 5,532,687.

[25] Chen, G., Tang, Y., Chen, Y., Li, Z., Guo, C., Fan, L., Bao, Y., Hu, X., & Klegseth, M. (2016). Smart Rock Technology for Real-Time Monitoring of Bridge Scour and Riprap Effectiveness - Design Guidelines and Visualization Tools. Department of Transportation.

[26] Chen, Y., Tang, F., Li, Z., Chen, G., & Tang, Y. (2018). Bridge scour monitoring using smart rocks based on magnetic field interference. Smart Materials and Structures, 27(8).

[27] Fisher, M., Atamturktur, S., & Khan, A. A. (2013). A novel vibration-based monitoring technique for bridge pier and abutment scour. Structural Health Monitoring, 12(2), 114-125. doi: 10.1177/1475921713476332

[28] Khan, A. A., Atamturktur, S., & Huriye, S. (2015). Real Time Measurement of Scour Depths Around Bridge Piers and Abutments.

[29] Atamturktur, S., & Khan, A. (2015). Vibration-Based Scouring Monitoring: Prototype Design, Laboratory Experiments and Field Deployment. Conference Proceedings of the Society for Experimental Mechanics Series, 7, 137-144.

[30] Hsieh, Y., Yang, C., Chen, S., Chen, C., Wu, C. M., & Huang, C. M. (2015). An accelerometer-based sensor system for real-time bridge scour monitoring. Sensors & Transducers, 194(11), 15-21.

[31] Chen, S. Y., Hsieh, Y. J., Yang, C. C., Wu, C. M., & Huang, C. M. (2016). A real-time bridge scour sensor system with accelerometers. Conference Record - IEEE Instrumentation and Measurement Technology Conference, 2016-July.

[32] Lin, Y. B., Lai, J. S., Chang, K. C., Chang, W. Y., Lee, F. Z., & Tan, Y. C. (2010). Using MEMS sensors in the bridge scour monitoring system. Journal of the Chinese Institute of Engineers, 33(1), 25-35.

[33] Ling, Y. B., Lai, J. S., Chang, K. C., Chang, W. Y., Lee, F. Z., & Tan, Y. C. (2010). Using MEMS sensors in the bridge scour monitoring system. Journal of the Chinese Institute of Engineers, 33(1), 25-35.

[34] Azhari, F., Scheel, P. J., & Loh, K. J. (2015). Monitoring bridge scour using dissolved oxygen probes. Structural Monitoring and Maintenance, 2(2), 145-164. doi: 10.12989/smm.2015.2.2.145

[35] Lu, J. Y., Hong, J. H., Su, C. C., Wang, C. Y., & Lai, J. S. (2008). Field measurements and simulation of bridge scour depth variations during floods. Journal of Hydraulic Engineering, ASCE, 134(6), 810-821.

[36] C-P Lin, K Wang, C-C Chung and Y-W Weng. (2017) New types of time domain reflectometry sensing waveguides for bridge scour monitoring, Smart Mater. Struct., vol. 26, 2017, p. 075014.

[37] Funderburk, M. L., Todd, M. D., Netchaev, A., and Loh, K. J. (2021) Active scour monitoring using ultrasonic time-domain reflectometry to detect a soil interface, in Sensors and Smart Structures Technologies for Civil, Mechanical, and Aerospace Systems.

[38] Funderburk, M. L., Tran, J., Todd, M. D., Netchaev, A., & Loh, K. J. (2022). Active scour monitoring using ultrasonic time domain reflectometry of buried slender sensors. Smart Materials and Structures, 31(1), 015045.

[39] Yu, X., & Yu, X. (2010). Laboratory evaluation of time-domain reflectometry for bridge scour measurement: Comparison with the ultrasonic method. Advances in Civil Engineering, 2010, 1-12.

[40] Dowding C. H., & Pierce, C. E. (1994). Use of time domain reflectometry to detect bridge scour and monitor pier movement. Proc Symp and Workshop on Time Domain Reflectometry in Envir. Infrastructure and Mining Applications, Northwestern University, Evanston, III, 579-587.

[41] Yankielun, N. E., & Zabilansky, L. (1999). Laboratory investigation of time-domain-reflectometry system for monitoring bridge scour. Journal of Hydraulic Engineering, 125(12), 1279-1284.

[42] Yu, X., & Zabilansky, L. J. (2006). Time domain reflectometry for automatic bridge scour monitoring. ASCE Geotechnical Special Publications, GeoShanghai, Shanghai, China.

[43] Azhari, F., & Loh, K. J. (2017). Laboratory validation of buried piezoelectric scour sensing rods. Structural Control and Health Monitoring, 24(9), 1-14.

[44] Zhang, W., Hao, H., Wu, J., Li, J., Ma, H., & Li, C. (2017). Detection of minor damage in structures with guided wave signals and nonlinear oscillator. Measurement.

[45] Rizzo, P., Han, J.-G., & Ni, X.-L. (2010). Structural Health Monitoring of Immersed Structures by Means of Guided Ultrasonic Waves. Journal of Intelligent Material Systems and Structures, 21(14), 1397-1407.

[46] Staszewski, W. J. (2005). Ultrasonic/guided waves for structural health monitoring. Key Engineering Materials, 293-294, 49-62.

[47] Rose, J. L. (2004). Ultrasonic guided waves in structural health monitoring. In Key engineering materials (Vol. 270, pp. 14-21). Trans Tech Publications Ltd.

[48] Yu, L., Santoni-Bottai, G., Xu, B., Liu, W., & Giurgiutiu, V. (2008). Piezoelectric wafer active sensors for in situ ultrasonic-guided wave SHM. Fatigue & Fracture of Engineering Materials & Structures, 31, 611-628.

[49] Rizzo, P., & di Scalea, F. L. (2006). Feature extraction for defect detection in strands by guided ultrasonic waves. Structural Health Monitoring, 5(3), 297-308.

[50] Staszewski, W., Boller, C., & Tomlinson, G. (2004). Health Monitoring of Aerospace Structures: Smart sensor technologies and signal processing. Munich, Germany: John Wiley & Sons.

[51] Sohn, H., Farrar, C. R., Hunter, N. F., & Worden, K. (2001). Structural health monitoring using statistical pattern recognition techniques. ASME Journal of Dynamic Systems, Measurement, and Control, 123, 706-711.

[52] Binotto, A., Castro, B. A., Santos, V. V. d., Rey, J. A. A., & Andreoli, A. L. (2020). A Comparison between Piezoelectric Sensors Applied to Multiple Partial Discharge Detection by Advanced Signal Processing Analysis. Eng. Proc., 2, 55.

[53] Wilkie, W. K., High, J., & Bockman, J. (2002). Reliability testing of NASA piezocomposite actuators. In Proceedings of the 8th International Conference on New Actuators (Actuator 2002) (pp. 225-229).

[54] Wilkie, W. K., Bryant, R. G., High, J. W., Fox, R. L., & Hellbaum, R. F. (2000). Low-cost piezocomposite actuator for structural control applications. Smart Structures and Materials: Industrial and Commercial Applications of Smart Structures Technologies (Vol. 3991, pp. 323-334). SPIE.

[55] Degefa, G. T., Płaczek, M. Ł., & Kokot, G. (2022). The Study of the Influence of Temperature and Low Frequency on the Performance of the Laminated MFC Piezoelectric Energy Harvester. Applied Sciences, 12(12), 12135.

[56] Lowe, M. J. S. (1995). Matrix techniques for modelling ultrasonic waves in multilayered media. IEEE Transactions on Ultrasonics, Ferroelectrics and Frequency Control, 42(4), 525-542.

[57] Chimenti, D. E. (1997). Guided waves in plates and their use in materials characterization. Applied Mechanics Reviews, 50(5), 247-284.

[58] Su, Z., Ye, L., & Lu, Y. (2006). Guided Lamb waves for identification of damage in composite structures: A review. Journal of Sound and Vibration, 295(3-5), 753-780.

[59] Rathod, V. T., Mahapatra, D. R., Jain, A., & Gayathri, A. (2010). Characterization of a large-area PVDF thin film for electro-mechanical and ultrasonic sensing applications. Sensors and Actuators A: Physical, 163(1), 164-171.

[60] Alleyne, D. N., & Cawley, P. (1992). The interaction of lamb waves with defects. IEEE Transactions on Ultrasonics, Ferroelectrics, and Frequency Control, 39(3), 381-397.

[61] Alleyne, D. N., & Cawley, P. (1992). Optimization of lamb wave inspection techniques. NDT & E International, 25(1), 11-22.

[62] Sodano, H. A., Park, G., & Inman, D. J. (2004). An investigation into the performance of macro-fiber composites for sensing and structural vibration applications. Mechanical Systems and Signal Processing, 18(3), 683-697.

[63] Mańka, M., Rosiek, M., Martowicz, A., Stepinski, T., & Uhl, T. (2013). Lamb wave transducers made of piezoelectric macro-fiber composite. Structural Control and Health Monitoring, 20(2), 173-184.

[64] Kundu, T., & Maslov, K. (1997). Material interface inspection by Lamb waves. International Journal of Solids and Structures, 34(29), 3885-3901.